Universiteit
Leiden
The Netherlands

Synthetic tools to study ubiquitin biology

Shahul Hameed, D.A.

Citation
Shahul Hameed, D. A. (2020, June 23). *Synthetic tools to study ubiquitin biology*. Retrieved from https://hdl.handle.net/1887/123181

Version:	Publisher's Version
License:	Licence agreement concerning inclusion of doctoral thesis in the Institutional Repository of the University of Leiden
Downloaded from:	https://hdl.handle.net/1887/123181

Note: To cite this publication please use the final published version (if applicable).

Cover Page

Universiteit Leiden

The handle http://hdl.handle.net/1887/123181 holds various files of this Leiden University dissertation.

Author: Shahul Hameed D.A.
Title: Synthetic tools to study ubiquitin biology
Issue Date: 2020-06-23

Chapter 4

Development of a Ubiquitin based probe for metalloprotease deubiquitinases

Adapted from:
Hameed, D.S., A. Sapmaz, L. Burggraaff, A. Amore, C.J. Slingerland, G.J.P. van Westen, and H. Ovaa, Development of Ubiquitin-Based Probe for Metalloprotease Deubiquitinases. Angew Chem Int Ed Engl, 2019. 58(41): p. 14477-14482.

Summary

The deubiquitinases (DUBs) are a family of enzymes that regulate the ubiquitin signalling cascade by removing ubiquitin from specific proteins in response to distinct signals. The DUBs that belong to the metalloprotease family (metalloDUBs) contain Zn^{2+} in its active site and are an integral part of distinct cellular protein complexes. Little is known about these enzymes due to the lack of specific probes because of the absence of a covalent enzyme-substrate intermediate complex during the deubiquitination process. Here we describe a Ub-based probe that contains a ubiquitin moiety modified at its C-terminus with a Zn^{2+} chelating group based on 8-mercaptoquinoline and that is modified at the N-terminus with a fluorescent tag or a pull-down tag. The probe is validated using Rpn11, a metalloDUB found in the 26S proteasome complex. This probe is able to bind to metalloDUBs and efficiently pulled down overexpressed metalloDUBs from HeLa cell lysate. Such probes may be used to study the mechanism of metalloDUBs in detail. This will allow us to better understand the biochemical processes of protein complexes that contain metalloDUBs.

Introduction

Ubiquitination is an important post-translational modification that plays a key role in many vital cellular events. [1-3] In this process, ubiquitin (Ub) is attached to a substrate protein by the concerted action of an enzyme cascade involving E1, E2 and E3 enzymes and it is removed by an enzyme family known as deubiquitinases (DUBs). [4-6] DUBs are classified into two main families: cysteine proteases and JAMM (JAB1/MPN /MOV34) metalloproteases.

The cysteine protease class of DUBs has a conserved cysteine residue at the active site that acts as a nucleophile [5, 7] and forms a covalent intermediate with the carbonyl group of the scissile amide bond in Ub conjugates. [8-10] This intermediate has been mimicked by several activity-based probes reported by us and others. [11-18]

Unlike cysteine protease DUBs, metalloprotease DUBs (metalloDUBs) do not form a covalent intermediate with their substrate. [1, 2, 19] MetalloDUBs contain a Zn^{2+} ion in their active site that coordinates two histidine residues and an aspartate residue. During deubiquitination by metalloDUBs, a non-covalent intermediate complex is formed between the active site of the enzyme and the scissile isopeptide bond of Ub. [20] This leads to the nucleophilic attack of the amide bond by a water molecule which is also coordinated to the active site Zn^{2+} ion. [21] This mechanism of action, lacking a covalent intermediate between substrate and enzyme, presents a challenge to develop a selective activity-based probe for metalloDUBs. [14, 22] By combining the chemical synthesis of Ub and a small molecule zinc chelator at the C-terminus of Ub, we developed a Ub-based probe that binds and pulls down metalloDUBs from cell lysate.

Results and discussion

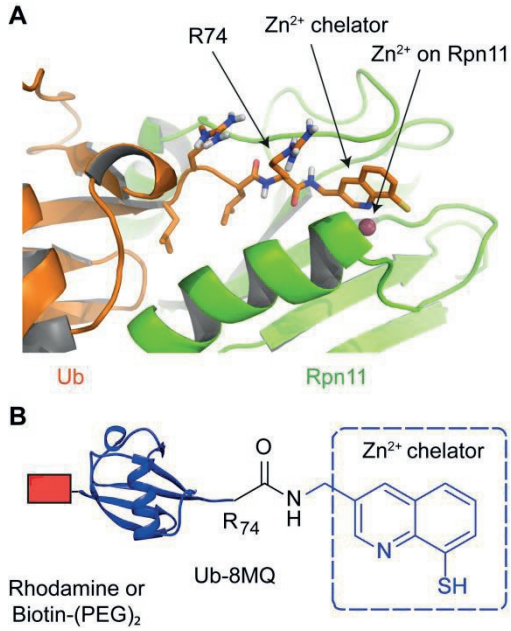

Figure 1: A: *Molecular docking using Prime showing Ub (1-74) coupled to our Zinc chelator at the C-terminus, which coordinated with* Zn^{2+} *on the active site of Rpn11 (PDB: 1UBQ, orange and 4O8X, green).* ***B:*** *The metalloDUB probe consists of an N-terminal dye or a tag, Ub (1-74) and the modified 8-MQ attached at the C-terminus of Arg74 of Ub.*

To develop a generic Ub-based probe, we relied on the information on structural similarity in the catalytic domain of the known metalloDUBs. The X-ray structures of AMSH, Rpn11/Rpn8 complex, and AMSH-LP/Lys63-linked diubiquitin complex reveal a similar active site configuration with a conserved Ub binding motif (Figure S1). [19, 23-25] To validate the inhibition and binding affinity of our Ub-based probe, we used recombinant *S.cerevisae* Rpn11/Rpn8 active enzyme complex which is a part of the 19S proteasome lid (Figure S2). [25] The activity of the recombinant Rpn11/Rpn8 enzyme complex was confirmed using a fluorogenic substrate (Ub-Rho) and a fluorescence polarization (FP) substrate Ub-FP (Ub-TAMRA-K48Ub-peptide). [26, 27] The rates of the enzyme reaction upon incubation with 1 μM of Rpn11/Rpn8 were calculated to be 0.075 $pmol.min^{-1}$ using Ub-Rho substrate and 0.42 $pmol.min^{-1}$ using Ub-TAMRA-K48Ub-peptide substrate (Figure S3, S4).

In order to chelate Zn^{2+} to the active site of metalloDUBs, we first used a hydroxamate moiety, that is known as a general metalloprotease inhibitor, [22, 28, 29] to the C-terminus of Ub. It has also been proposed that Ub containing N-hydroxy isopeptide at the C-terminal glycine may inhibit metalloDUBs. [30] We found that Ub-hydroxamic acid derivatives failed to inhibit Rpn11 (Figure S5). This necessitated a different approach for developing a probe for metalloDUBs.

Many molecules have been reported as zinc chelating agents and among them, 8-mercaptoquinoline (8-MQ) was reported as an efficient chelator. [31, 32] Furthermore, 8-

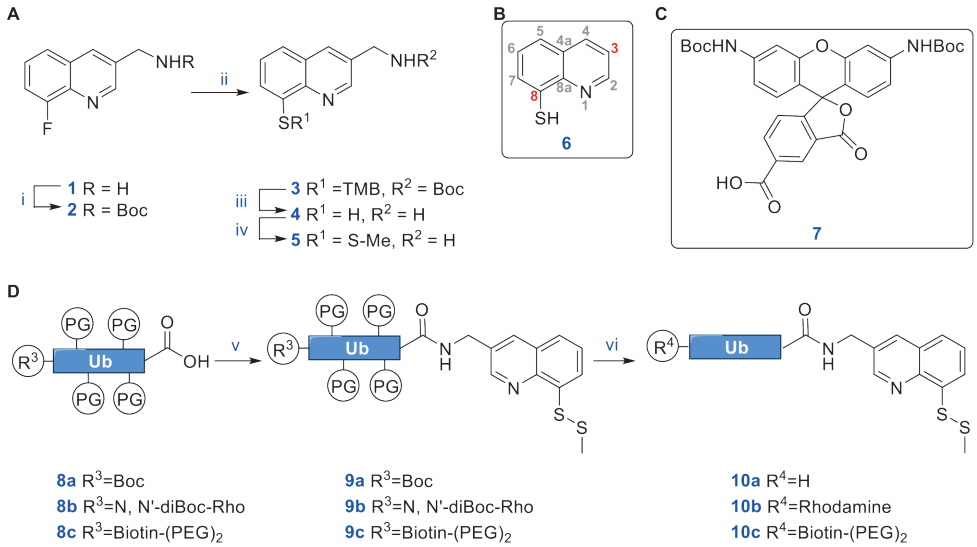

Scheme 1 A: *i) Di-tert-butyl dicarbonate, DIPEA, CH_3CN, room temperature; ii) TMB-thiol, NaH, THF, 60 °C; iii) TFA, TES, H_2O; iv) MMTS, MeOH.* ***B:*** *Chemical structure of 8-quinolium thiolate (6) and its carbon positions are indicated in numbers.* ***C:*** *N,N'-diBoc protected rhodamine (7) used in Fmoc-SPPS of rhodamine labeled Ub derivatives.* ***D:*** *v) 5, HBTU, HOBT, DIPEA, room temperature (PG- protecting groups); vi) TFA, TIPS, Phenol, H_2O.*

MQ and its derivatives were also reported as a specific inhibitor for metalloDUBs like Rpn11 and AMSH. [32, 33] In addition, it is known that a modification at position 3 (Scheme 1B, **6**) of this molecule will not diminish its inhibitory potential. [34] Hence, an 8-MQ derivative modified with an amino group at position 3 was subsequently synthesized as zinc-binding group (ZBG).

We prepared the 8-MQ derivative **5** (Scheme 1A, Scheme S1) starting from commercially available (8-fluoroquinolin-3-yl) methanamine **1**. After tert-butoxycarbonyl (Boc) protection, the fluorine atom was substituted with trimethoxybenzyl (TMB) thiol and afforded the protected thiol **3**. After acid deprotection of the thiol, compound **4** was obtained. We observed that **4** could dimerize as a disulfide and that this leads to difficulties during purification. Hence, we protected the free thiol as a thio-methyl disulfide **5** which was then purified and used in further peptide-coupling reactions.

In order to precisely accommodate our ZBG on the C-terminus of Ub, we performed molecular docking analysis. For this purpose, we used the known X-ray crystal structure of Rpn11/Rpn8 (PDB: 4O8X) and Ub (PDB: 1UBQ). [25, 35] Among all the models tested, we arrived at optimal binding when our ZBG was attached at the C-terminus of Arg74 of Ub (Figure 1A, S6). Therefore, we designed our metalloDUB probe containing an N-terminally modified Ub (1-74) attached with 3-aminomethyl 8-mercapto quinoline at its C-terminus

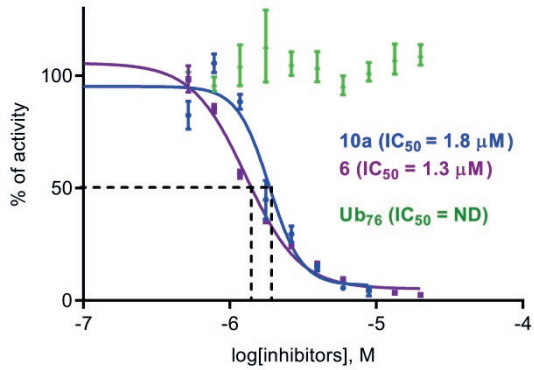

***Figure 2**: Rpn11 inhibition by **6**, **10a** and Ub_{76}. IC_{50} curve of Ub-Rho hydrolysis in a typical fluorogenic assay. In this assay, compound **6** was also taken along, which shows an IC_{50} of about 1.3 μM while **10a** shows an IC_{50} of 2 μM. Full length Ub did not inhibit the enzyme.*

(Figure 1B).

We synthesized fully protected Ub74 containing either protected rhodamine (**7**, Scheme 1C) or Biotin-$(PEG)_2$ or a Boc protecting group at its N-terminus by Fmoc-based SPPS on a 2-chlorotrityl resin. [36-38] After selective C-terminal cleavage using 20% hexafluoroisopropanol (HFIP) in dichloromethane (DCM), we obtained fully protected Ub containing a free C-terminal carboxylate group and either a bis-Boc-rhodamine or Biotin-$(PEG)_2$ or a Boc protecting group on the N-terminus (**8a, 8b, 8c**, Scheme 1C). The amino group of compound **5** was then coupled to the C-terminal carboxylate of Ub74 to yield **9a, 9b** and **9c**. After global deprotection, the final products were purified using reversed-phase HPLC followed by size exclusion chromatography to afford labelled or unlabeled versions of Ub-8MQ reagents **10a, 10b** and **10c**. The disulfide protected Ub-8MQ was reduced using TCEP prior to use and we observed only a slight decrease in the activity of Rpn11/Rpn8 upon the addition of TCEP (Figure S7, S8). Commercially available 8-quinoliniumthiolate (**6**, Scheme 1B) was used as a positive control in our assay.

Inhibition of Rpn11/Rpn8 by **10a** was then tested using both Ub-rhodamine and Ub-fluorescence polarization (Ub-FP) assay reagents as substrates. [25] We observed that both **6** and **10a** were able to inhibit Rpn11/Rpn8 with an IC_{50} of about 2 μM (Figure 2, S9). To discern whether this inhibition is reversible or irreversible, we followed two different approaches. First, we performed a time-course pre-incubation assay using EDTA as a control. EDTA is known to strip Zn^{2+} from many proteins and therefore acts as an irreversible inhibitor. [39] The activity assay showed that inhibition by EDTA increased with longer pre-incubation times. On the other hand, **10a** initially decreased the enzyme activity and then maintained the inhibition irrespective of longer pre-incubation times (Figure S10), suggesting that unlike EDTA, the reagent **10a** reversibly binds by coordinating to the active site of the Rpn11/Rpn8 enzyme.

Secondly, we carried out an activity recovery assay using $ZnSO_4$. After pre-incubating Rpn11/Rpn8 with **6** or **10a**, we added an excess of $ZnSO_4$ to the assay buffer and incubated further. Then, we tested the activity of the enzyme using an FP assay. We observed that the enzyme Rpn11/Rpn8, pre-incubated with **6** and **10a**, completely recovered its activity after adding $ZnSO_4$ to the buffer (Figure S11), implying that the chelating groups in **6** and **10a** bind to Zn^{2+} in a reversible manner.

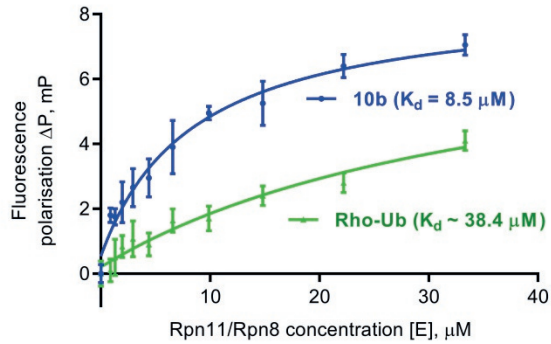

Figure 3: *Fluorescence polarization based binding assay between* ***10b*** *and Rpn11/Rpn8. A typical FP-based binding between Rho-Ub and* ***10b*** *was measured against an unlabelled Rpn11/Rpn8.* ***10b*** *has an almost 5 times higher affinity compared to full length Ub*

In order to establish the binding affinity of **10a** with Rpn11/Rpn8, we used fluorescently labelled derivative **10b** as a fluorescence polarization (FP) probe. [40] We measured the binding of unlabeled Rpn11/Rpn8 using both **10b** and rhodamine-labelled Ub_{76} in a typical

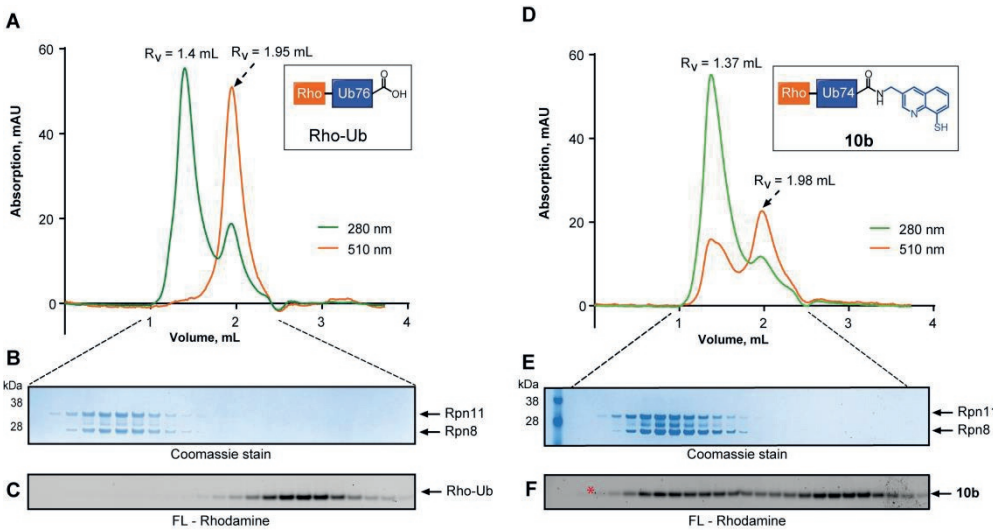

Figure 4: *Co-elution assay.* ***A:*** *Co-elution pattern of RhoUb (inset) with an Rpn11/Rpn8 complex by SEC.* ***B:*** *The fractions from the column in A were used for analysis by SDS-PAGE (coomassie stain).* ***C:*** *The same gel (B) analyzed using fluorescence at the emission wavelength of rhodamine.* ***D:*** *Co-elution pattern of* ***10b*** *(inset) with Rpn11/Rpn8 by SEC.* ***E:.*** *The fractions from the column in D were used in a SDS-PAGE and analyzed by coomassie stain.* ***F:*** *The same gel (E) analyzed using fluorescence at the emission wavelength of rhodamine. The red asterix marks the presence of rhodamine signal from the* ***10b*** *probe in the fractions from D.*

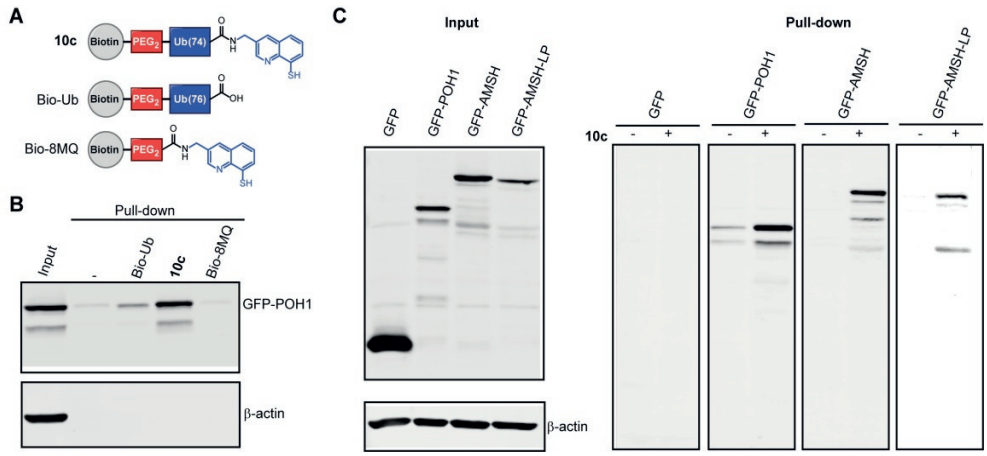

Figure 5: *Pull-down using* ***10c****. **A:** Schematic representation of pull-down reagents used in the assay. **B:** Western Blot analysis of pull-down from cell lysate of HeLa cells overexpressing GFP-POH1.* ***10c*** *efficiently pulled-down GFP-POH1 compared with Bio-Ub or Bio-8MQ alone. **C:** Using* ***10c****, other metalloDUBs like GFP-AMSH and GFP-AMSHLP were also pulled-down from overexpressing HeLa cell lysate.*

FP-binding experiment. In our assays, the reagent **10b** showed a binding affinity of 8.5 μM. On the other hand, full-length Ub binds to Rpn11/Rpn8 with a K_d of 38 μM (Figure 3). This shows that the reagent **10b** can tightly bind to the Rpn11/Rpn8 complex compared to wild-type Ub.

Next, we tested the formation of a stable complex between our probe and Rpn11/Rpn8 in a retention-time shift assay on a size exclusion chromatography (SEC) column. In order to visualize the co-elution of Rpn11/Rpn8 with our probe, we used **10b** and rhodamine-labelled Ub_{76} such that the absorption signal of rhodamine was followed. In addition, the fractions from the SEC column were visualized by SDS-PAGE both by in-gel fluorescence imaging and by Coomassie staining.

Having established the retention times of Rpn11/Rpn8, rhodamine-labelled Ub_{76} and **10b** separately (Figure S12A, S12B and S12C), we incubated Rpn11/Rpn8 with an excess of either rhodamine-labelled Ub_{76} or **10b** and used SEC to determine whether a complex is formed between them. We observed that rhodamine-labelled Ub_{76} does not co-elute with the Rpn11/Rpn8 (Figure 4A). Interestingly, incubating **10b** with Rpn11/Rpn8 resulted in co-elution implying that the Ub74-8MQ forms a tight complex with the enzyme (Figure 4B). This shows that the Ub-8MQ reagent can effectively bind Rpn11/Rpn8.

After determining that Ub-8MQ probe was able to bind efficiently with Rpn11/Rpn8 in our in vitro assays, we examined whether metalloDUBs in cell lysate can be captured by our probe. For this purpose, we synthesized a biotinylated Ub-8MQ probe (**10c**, Scheme 1D) and used biotin-Ub and biotin-8MQ as controls (Figure 5A). Cell lysate prepared from HeLa cells overexpressing GFP-POH1 (human homolog of Rpn11) was incubated with **10c**, along with biotin-Ub and biotin-8MQ and streptavidin beads were used to pull-down GFP-POH1 bound to our probe. As expected, **10c** was able to pull down GFP-POH1 with higher efficiency than biotin-Ub or biotin-8MQ alone (Figure 5B). Even though the IC_{50} values of **10a** and 8MQ are similar (Figure 2), our pull-down experiments show that the Ub handle is indispensable to tightly interact with metalloDUBs.

To determine whether this is true for other known metalloDUBs, we overexpressed GFP-

POH1, GFP-AMSH and GFP-AMSHLP in HeLa cells and carried out a pull-down assay using **10c**. As expected, **10c** was able to pull-down metalloDUBs from cell lysate (Figure 5C). This shows that our probe can also be used to pull-down other metalloDUBs from complex mixtures in human cells.

Conclusion

In conclusion, a zinc chelator was synthesized and coupled to the C-terminal end of Ub to generate a first-generation metalloDUB probe. In our assays, the Ub_{74}-8MQ reagent was able to inhibit the activity of Rpn11/Rpn8 better than full-length Ub alone. In addition, the Ub74-8MQ reagent can form a tight complex with Rpn11/Rpn8. A biotinylated metalloDUB probe was also able to pull-down POH1, AMSH and AMSH-LP from HeLa cell lysates. The metalloprotease DUBs, in general, share similar structural features in the active site of the enzyme and exist as a part of the multi-molecular protein complex. [6] [41-44] Thus, reagents like the one described here may be used as a probe to detect the activity of metalloDUBs and their associated proteins.

Acknowledgements

We would like to thank Henk Hilkmann and Dris el Atmioui for peptide synthesis; Remco Merkx for providing TMB-thiol reagent; Andreas Martin for providing the plasmid for Rpn11/Rpn8 heterodimer expression; Paul Geurink for providing bis-Boc-protected rhodamine, Ub-FP assay reagent and for critical reading of the manuscript. Work in the H.O lab is funded by an NWO (VICI grant 724.013.002) to H.O and an ITN fellowship to A.S.

References

1. Ambroggio, X.I., D.C. Rees, and R.J. Deshaies, *JAMM: a metalloprotease-like zinc site in the proteasome and signalosome.* PLoS Biol, 2004. **2**(1): p. 113-119.
2. Kikuchi, K., et al., *Identification of AMSH-LP containing a Jab1/MPN domain metalloenzyme motif.* Biochem Biophys Res Commun, 2003. **306**(3): p. 637-43.
3. Verma, R., et al., *Role of Rpn11 metalloprotease in deubiquitination and degradation by the 26S proteasome.* Science, 2002. **298**(5593): p. 611-5.
4. Hershko, A. and A. Ciechanover, *The ubiquitin system.* Annu Rev Biochem, 1998. **67**: p. 425-79.
5. Komander, D., *Mechanism, specificity and structure of the deubiquitinases.* Subcell Biochem, 2010. **54**: p. 69-87.
6. Komander, D., M.J. Clague, and S. Urbe, *Breaking the chains: structure and function of the deubiquitinases.* Nat Rev Mol Cell Biol, 2009. **10**(8): p. 550-63.
7. Abdul Rehman, S.A., et al., *MINDY-1 Is a Member of an Evolutionarily Conserved and Structurally Distinct New Family of Deubiquitinating Enzymes.* Mol Cell, 2016. **63**(1): p. 146-55.
8. Hu, M., et al., *Crystal structure of a UBP-family deubiquitinating enzyme in isolation and in complex with ubiquitin aldehyde.* Cell, 2002. **111**(7): p. 1041-54.
9. Kessler, B.M., *Putting proteomics on target: activity-based profiling of ubiquitin and ubiquitin-like processing enzymes.* Expert Rev Proteomics, 2006. **3**(2): p. 213-21.
10. Komander, D. and D. Barford, *Structure of the A20 OTU domain and mechanistic insights into deubiquitination.* Biochem J, 2008. **409**(1): p. 77-85.
11. Hameed, D.S., A. Sapmaz, and H. Ovaa, *How Chemical Synthesis of Ubiquitin Conjugates Helps To Understand Ubiquitin Signal Transduction.* Bioconjug Chem, 2016.
12. Ekkebus, R., et al., *On terminal alkynes that can react with active-site cysteine nucleophiles in proteases.* J Am Chem Soc, 2013. **135**(8): p. 2867-70.
13. Sommer, S., et al., *Covalent inhibition of SUMO and ubiquitin-specific cysteine proteases by an in situ thiol-alkyne addition.* Bioorg Med Chem, 2013. **21**(9): p. 2511-7.
14. Hewings, D.S., et al., *Activity-based probes for the ubiquitin conjugation-deconjugation machinery: new chemistries, new tools, and new insights.* The FEBS Journal, 2017: p. 1555-1576.
15. Gopinath, P., et al., *Chemical and semisynthetic approaches to study and target deubiquitinases.* Chem Soc Rev, 2016. **45**(15): p. 4171-98.
16. Borodovsky, A., et al., *Chemistry-based functional proteomics reveals novel members of the deubiquitinating enzyme family.* Chem Biol, 2002. **9**(10): p. 1149-59.
17. Lam, Y.A., et al., *Editing of ubiquitin conjugates by an isopeptidase in the 26S proteasome.* Nature, 1997. **385**(6618): p. 737-40.
18. Meledin, R., et al., *Activity-Based Probes Developed by Applying a Sequential Dehydroalanine Formation Strategy to Expressed Proteins Reveal a Potential alpha-Globin-Modulating Deubiquitinase.* Angew Chem Int Ed Engl, 2018. **57**(20): p. 5645-5649.
19. Davies, C.W., et al., *Structural and thermodynamic comparison of the catalytic domain of AMSH and AMSH-LP: nearly identical fold but different stability.* J Mol Biol, 2011. **413**(2): p. 416-29.
20. Clague, M.J., et al., *Deubiquitylases from genes to organism.* Physiol Rev, 2013. **93**(3): p. 1289-315.

21. Tran, H.J., et al., *Structure of the Jab1/MPN domain and its implications for proteasome function.* Biochemistry, 2003. **42**(39): p. 11460-5.
22. Saghatelian, A., et al., *Activity-based probes for the proteomic profiling of metalloproteases.* Proc Natl Acad Sci U S A, 2004. **101**(27): p. 10000-5.
23. Pathare, G.R., et al., *Crystal structure of the proteasomal deubiquitylation module Rpn8-Rpn11.* Proc Natl Acad Sci U S A, 2014. **111**(8): p. 2984-9.
24. Sato, Y., et al., *Structural basis for specific cleavage of Lys 63-linked polyubiquitin chains.* Nature, 2008. **455**(7211): p. 358-62.
25. Worden, E.J., C. Padovani, and A. Martin, *Structure of the Rpn11-Rpn8 dimer reveals mechanisms of substrate deubiquitination during proteasomal degradation.* Nat Struct Mol Biol, 2014. **21**(3): p. 220-7.
26. Hassiepen, U., et al., *A sensitive fluorescence intensity assay for deubiquitinating proteases using ubiquitin-rhodamine110-glycine as substrate.* Anal Biochem, 2007. **371**(2): p. 201-7.
27. Geurink, P.P., et al., *A general chemical ligation approach towards isopeptide-linked ubiquitin and ubiquitin-like assay reagents.* Chembiochem, 2012. **13**(2): p. 293-7.
28. Morell, M., et al., *Coupling protein engineering with probe design to inhibit and image matrix metalloproteinases with controlled specificity.* J Am Chem Soc, 2013. **135**(24): p. 9139-48.
29. Sieber, S.A., et al., *Proteomic profiling of metalloprotease activities with cocktails of active-site probes.* Nat Chem Biol, 2006. **2**(5): p. 274-81.
30. Maity, S.K., S. Ohayon, and A. Brik, *Synthesis of N-Hydroxy Isopeptide Containing Proteins.* Org Lett, 2015. **17**(14): p. 3438-41.
31. Kawai, K. and N. Nagata, *Metal-ligand interactions: an analysis of zinc binding groups using the Protein Data Bank.* Eur J Med Chem, 2012. **51**: p. 271-6.
32. Perez, C., et al., *Discovery of an Inhibitor of the Proteasome Subunit Rpn11.* J Med Chem, 2017.
33. Li, J., et al., *Capzimin is a potent and specific inhibitor of proteasome isopeptidase Rpn11.* Nat Chem Biol, 2017. **13**(5): p. 486-493.
34. Zhou, H., Parlati, F., Roufflet, M., Emberley, E., Deshaies, R., Cohen, S., WO/2012/158435, *COMPOSITIONS AND METHODS FOR JAMM PROTEIN INHIBITION*. 2012.
35. Vijay-Kumar, S., C.E. Bugg, and W.J. Cook, *Structure of ubiquitin refined at 1.8 A resolution.* J Mol Biol, 1987. **194**(3): p. 531-44.
36. El Oualid, F., et al., *Chemical synthesis of ubiquitin, ubiquitin-based probes, and diubiquitin.* Angew Chem Int Ed Engl, 2010. **49**(52): p. 10149-53.
37. Shanmugham, A., et al., *Nonhydrolyzable ubiquitin-isopeptide isosteres as deubiquitinating enzyme probes.* J Am Chem Soc, 2010. **132**(26): p. 8834-5.
38. Geurink, P.P., et al., *Development of Diubiquitin-Based FRET Probes To Quantify Ubiquitin Linkage Specificity of Deubiquitinating Enzymes.* Chembiochem, 2016. **17**(9): p. 816-20.
39. Nyborg, J.K. and O.B. Peersen, *That zincing feeling: the effects of EDTA on the behaviour of zinc-binding transcriptional regulators.* Biochem J, 2004. **381**(Pt 3): p. e3-4.
40. Buchli, R., et al., *Real-time measurement of in vitro peptide binding to soluble HLA-A*0201 by fluorescence polarization.* Biochemistry, 2004. **43**(46): p. 14852-63.
41. Cooper, E.M., et al., *K63-specific deubiquitination by two JAMM/MPN+ complexes: BRISC-associated Brcc36 and proteasomal Poh1.* EMBO J, 2009. **28**(6): p. 621-31.

42. Cope, G.A., et al., *Role of predicted metalloprotease motif of Jab1/Csn5 in cleavage of Nedd8 from Cul1.* Science, 2002. **298**(5593): p. 608-11.
43. McCullough, J., et al., *Activation of the endosome-associated ubiquitin isopeptidase AMSH by STAM, a component of the multivesicular body-sorting machinery.* Curr Biol, 2006. **16**(2): p. 160-5.
44. Yao, T. and R.E. Cohen, *A cryptic protease couples deubiquitination and degradation by the proteasome.* Nature, 2002. **419**(6905): p. 403-7.

Supplementary figures

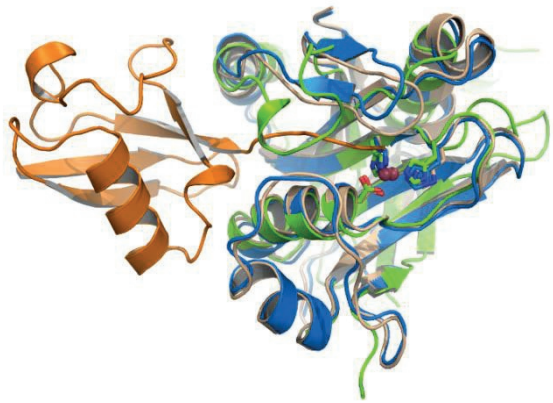

***Figure S1**: X-ray structures showing the catalytic domain of AMSH in complex with Ub (Blue for AMSH and orange for Ub, PDB: 2ZNV), overlaid on the catalytic domains of AMSH-LP (Brown, PDB: 3RZU) and Rpn11 (Green, PDB:4O8X). The active site containing two histidine residues and the aspartate residue is shown in a stick representation while the Zn^{2+} is shown in dark pink colour. The C-terminus of Ub is accommodated into a groove that extends into the active-site residues and the Zn^{2+} ion.*

***Figure S2**: Coomassie-stained image of the SDS-PAGE gel containing the eluted fractions of Rpn11/Rpn8 heterodimer complex from size-exclusion chromatography. Rpn11/Rpn8 heterodimer was expressed into BL21 E.coli cells and eluted from the cell lysate using TALON Metal Affinity Resin™. The heterodimer complex of Rpn11/Rpn8 was purified by size-exclusion chromatography on a HiLoad 16/60 Superdex 200 pg column (GE Life Sciences). Pure fractions were pooled, concentrated and stored at -80 ºC for future use.*

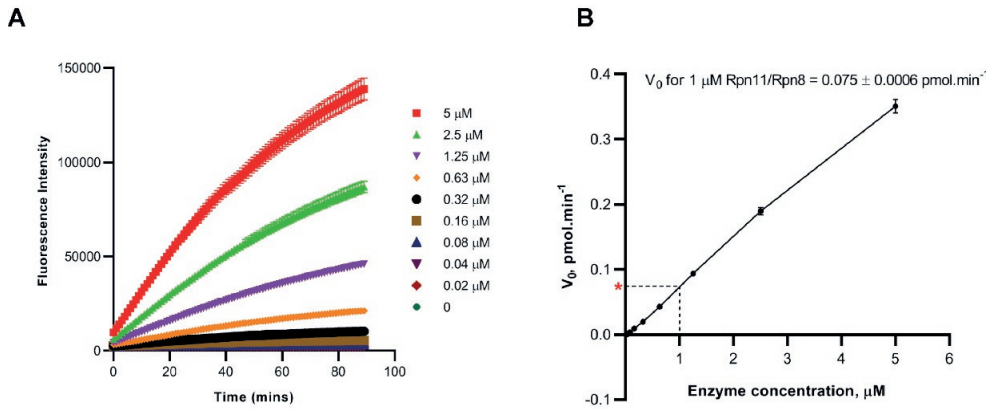

***Figure S3**: **A**: The activity of the purified Rpn11/rpn8 enzyme complex was measured using the rate of hydrolysis of Ub-Rho assay reagent. Rpn11/Rpn8 heterodimer complex was taken at different concentrations ranging from 5 μM down to 0.01 μM and used against 2 μM of Ub-Rho substrate. **B:** An enzyme concentration vs initial enzyme-velocity plot showing an almost linear correlation. The red asterisk (*) shows the value of V_0 for 1 μM of Rpn11/Rpn8 used in the assay.*

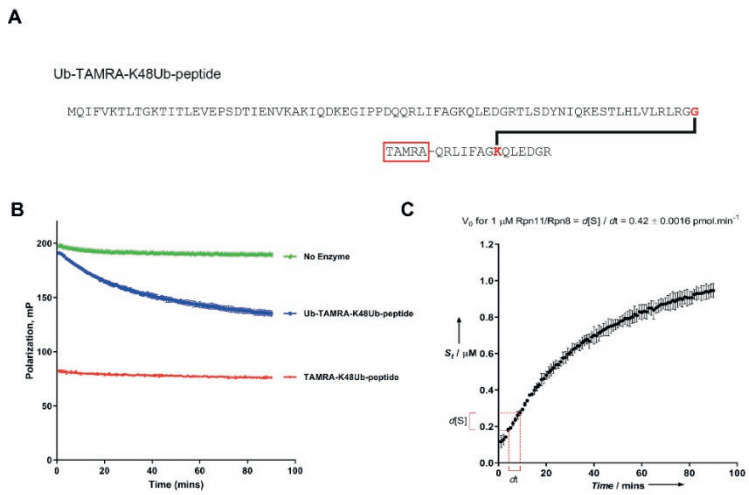

***Figure S4: A:** Sequence of the FP assay reagent that was chosen based on Rpn11/Rpn8 preference towards K48 linked diUbs [1]. The FP assay reagent contains full-length Ub ligated with a TAMRA-labelled peptide containing residues 41-54 of Ub. **B:** The hydrolysis of Ub- FP assay reagent by Rpn11/Rpn8, measured using a TAMRA-based fluorescence polarization assay. Upon hydrolysis by Rpn11, the TAMRA-labeled peptide is released, and the fluorescence polarization was measured on the Y-axis against time on the X-axis. [2] **C:** The rate of hydrolysis of the FP assay reagent in Figure S4B were calculated. The rate of consumption of the substrate was plotted on Y-axis against time on X-axis. The initial rate of enzyme activity (V_0) was calculated from the slope of the linear part of the curve, shown in red.*

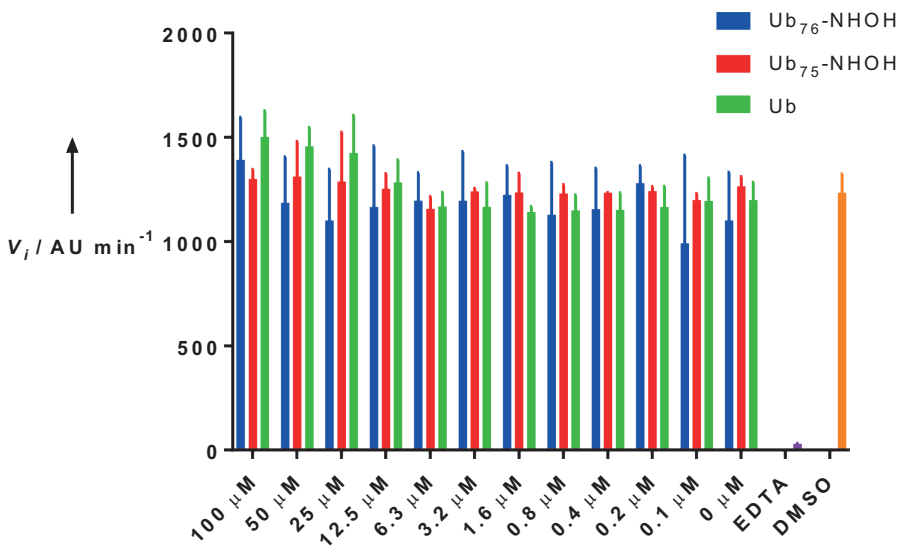

***Figure S5**: Two different lengths of ubiquitin-hydroxamate were used at different concentrations in a Ub-Rho assay to test for inhibition of Rpn11/Rpn8. Full-length Ub was used as a control. Ub_{76}, Ub_{75}-NHOH and Ub_{76}-NHOH did not inhibit the Rpn11/Rpn8 enzyme even at the highest concentrations used here.*

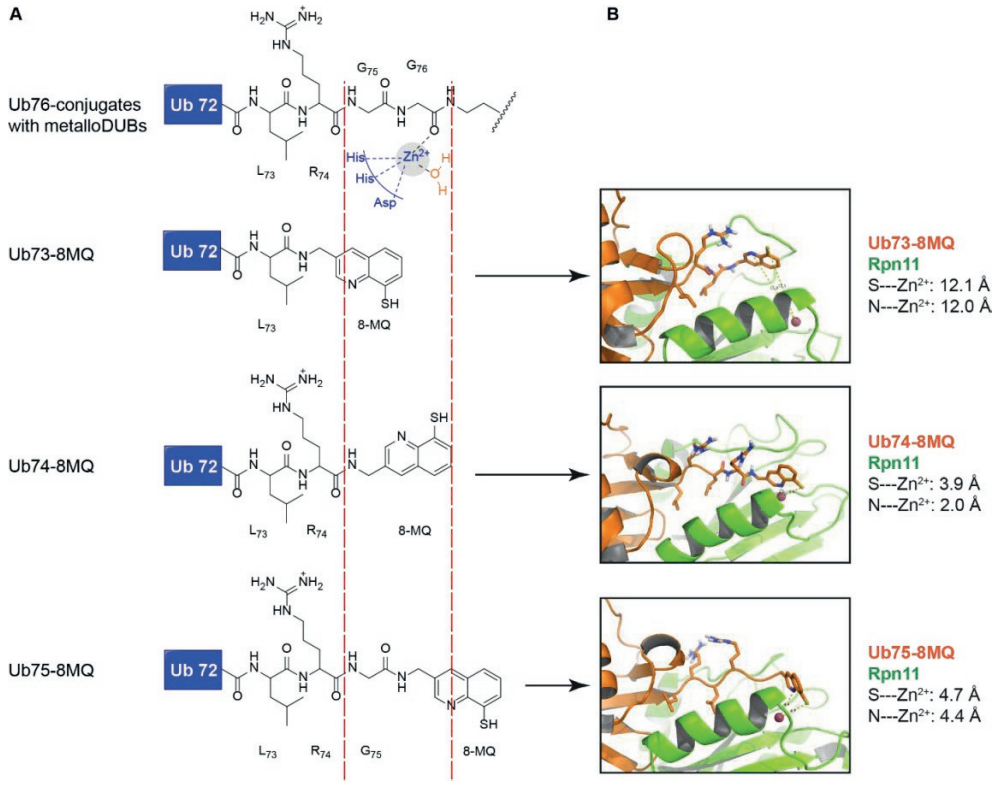

Figure S6: A: *Design of Ub74-8MQ. Comparing Ub76 with Zn^{2+} of metalloDUB, Ub73-8MQ falls short of a length, while Ub75-8MQ is longer. Ub74-8MQ provides the exact length that matches with Ub76.* ***B:*** *Molecular docking using Rpn11 (green, PDB: 4O8X) and different lengths of Ub-8MQ (orange, based on 1UBQ and 8MQ). Distance calculations from Zn^{2+} to the coordinating elements namely the Sulphur and Nitrogen of 8MQ shows that Ub74-8MQ is much closely positioned for coordinating with Zn^{2+} on the active site of Rpn11.*

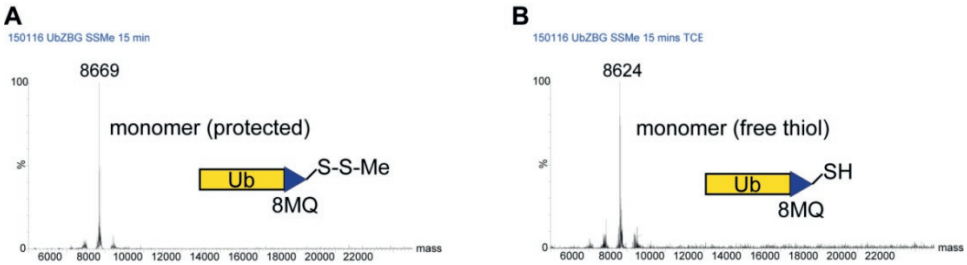

Figure S7: A: *Deconvoluted mass spectrum data for* ***10a*** *(Ub_{74}-8MQ) protected as a disulfide of methyl thiol. ESI-Mass [M+H] for protected* ***10a*** *- Expected: 8666 / Found: 8669.* ***B:*** *Deconvoluted mass spectrum data for* ***10a*** *after the addition of 25 mM TCEP for 15 minutes at RT. ESI-Mass [M+H] for reduced* ***10a*** *- Expected: 8622 / Found: 8624.*

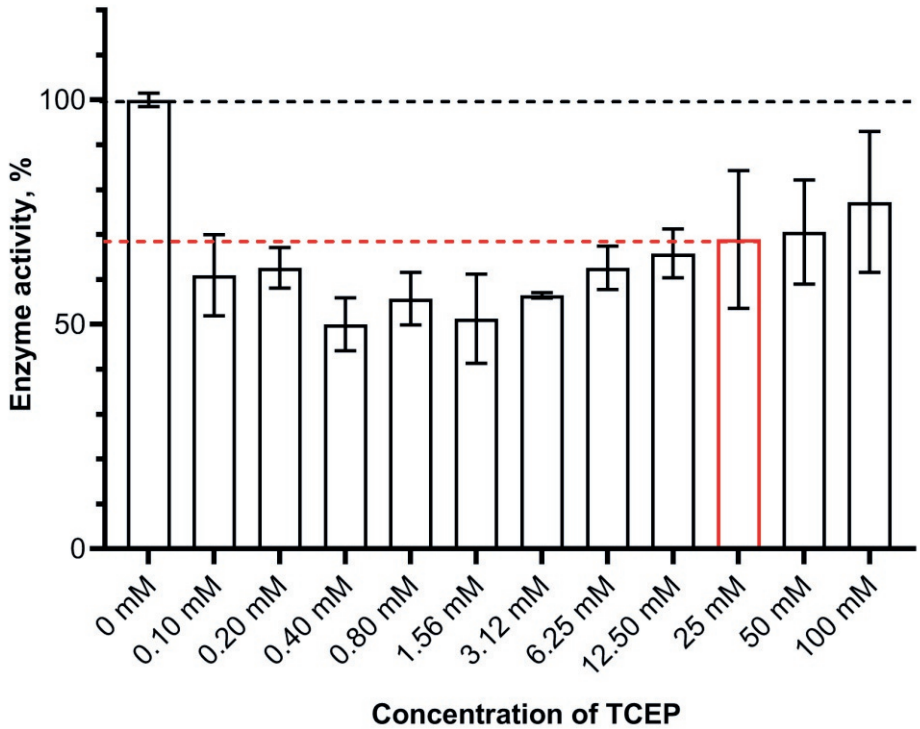

Figure S8*: The influence of TCEP on Rpn11/Rpn8 activity at different concentrations was measured using Ub-rho assay. Although there is a general reduction in the enzyme activity by approximately 30%, the enzyme was active even at the concentrations of 100 mM TCEP. For practical purposes, we used 25 mM TCEP in our assay buffers in order to reduce* ***10a, 10b and 10c****.*

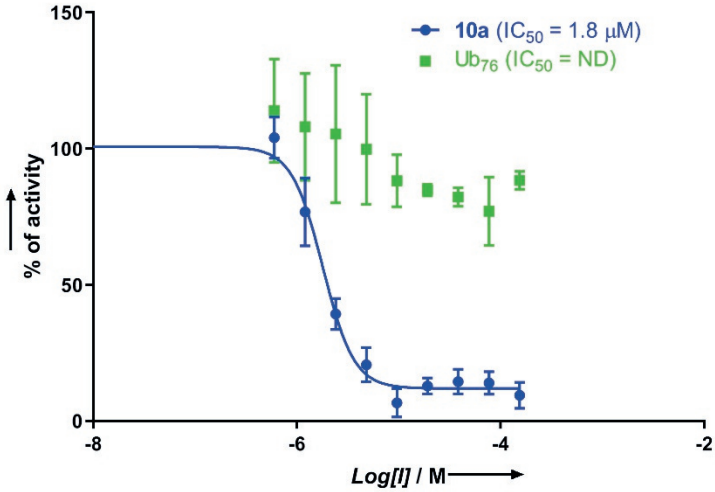

***Figure S9**: The Ub-FP assay reagent (Figure S4) was used in an FP assay and the IC_{50} values of **10a** on Rpn11/Rpn8 were calculated. The IC_{50} values were comparable to the results in the Ub-Rho assay (Figure 2).*

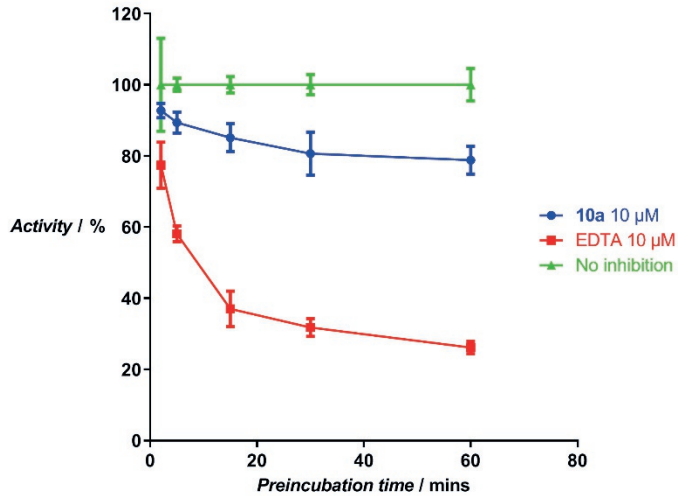

***Figure S10**: In this assay, Rpn11/Rpn8 and **10a** or EDTA were pre-incubated at different time durations before adding Ub-rhodamine substrate. EDTA progressively increased the inhibition of Rpn11/Rpn8 on increasing the incubation time while **10a** showed no such correlation, although a minimal decrease was initially observed. Normalized enzyme activity was shown in the Y-axis and different pre-incubation time is plotted in the X-axis.*

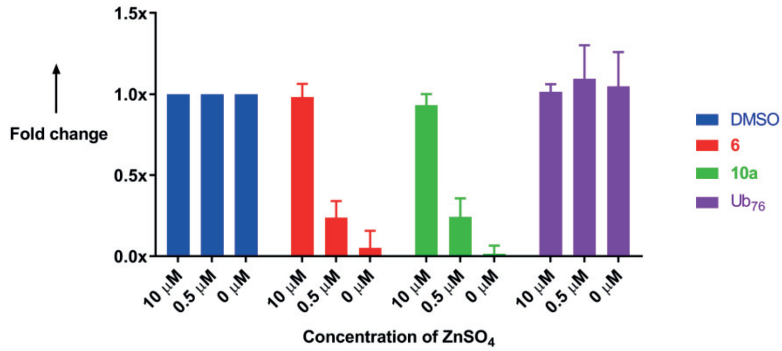

Figure S11*: Rpn11/Rpn8 was pre-incubated with either 5 μM 8-MQ, 10 μM* ***10a*** *or 10 μM* Ub_{76} *for 30 minutes at RT. Later, 10 μM, 0.5 μM or 0 μM* $ZnSO_4$ *was added to the FP assay buffer for 15 minutes and then the activity of the enzyme was measured using K48 FP reagent. The initial velocity of the enzyme for different inhibitors was normalized to DMSO control samples. Rpn11/Rpn8 was able to recover its activity after incubating with higher concentrations of* $ZnSO_4$.

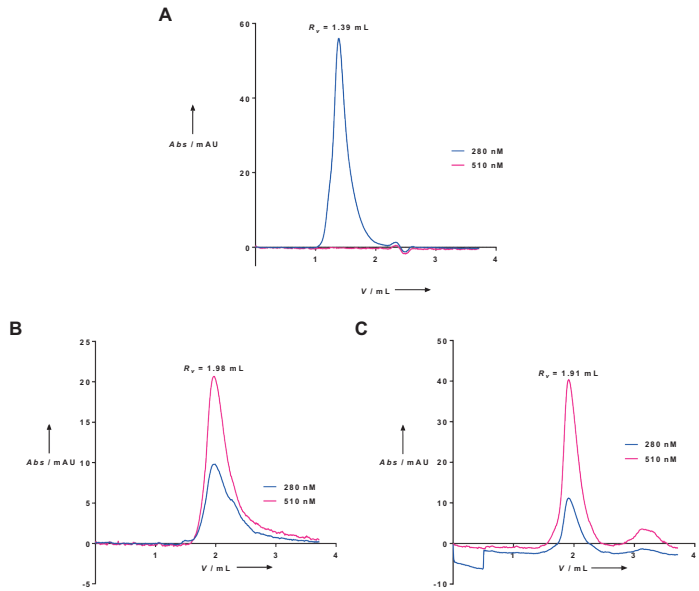

Figure S12: A: *1 μM of Rpn11/Rpn8 was loaded on S75/200 column and the absorbance at 280 nm and 510 nm was measured. The retention time for Rpn11/Rpn8 was about 1.39 mL.* ***B:*** *8 μM of* ***10b*** *was loaded on S75/200 column and the absorbance at 280 nm and 510 nm was measured. The retention time for* ***10b*** *was about 1.98 mL.* ***C:*** *8 μM of RhoUb was loaded on S75/200 column and the absorbance at 280 nm and 510 nm was measured. The retention time for RhoUb was about 1.91 mL.*

Synthesis scheme of 8-mercapto quinolone 3 methylamine

General: All commercial materials (Aldrich, Fluka, Novabiochem) were used without further purification. All solvents were reagent grade or HPLC grade. DCM and THF were passed through a column of alumina. Unless stated otherwise, reactions were performed under inert atmospheres. NMR spectra (1H and 13C) were recorded with a Bruker Avance 300 spectrometer, referenced to TMS or residual solvent. LC-MS analysis was performed with a system containing a Waters 2795 separation module (Alliance HT), Waters 2996 Photodiode Array Detector (190–750 nm), Waters Alltima C18 (2.1 x 100 mm) or Phenomenex Kinetex XB-C18 (2.1 x 50 mm) reversed-phase column and a MicromassLCT-TOF mass spectrometer. Samples were run at 0.40 mL min x 1(Waters C18) or 0.80 mL min x 1 (Kinetex C18) with the use of a gradient of two mobile phases: A) aq. formic acid (0.1 %), and B) formic acid in CH_3CN (0.1 %). Data processing was performed with the aid of Waters MassLynx 4.1 software (deconvolution with Maxent1 function). Preparative HPLC was performed with a Shimadzu LC-20AD/T instrument fitted with a C18 Vydac column (Grace Davison Discovery Sciences) with the use of gradient elution [mobile phases: A) aq. TFA (0.05 %) and B) TFA in CH_3CN (0.05 %)].

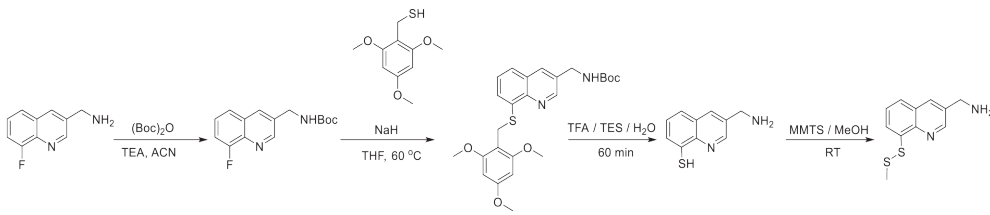

Scheme S1: Synthesis of the zinc chelating molecule (8-(methyldisulfaneyl)quinolin-3-yl)methanamine

Synthesis of tert-butyl ((8-fluoroquinolin-3-yl)methyl) carbamate (2). Commercially available (8-fluoroquinolin-3-yl)methanamine (**1**, 465 mg, 2.84 mmol) was dissolved in acetonitrile (25 mL). To this, a solution of TEA (2 eq, 5.68 mmol, 756.5 µL) was added drop wise. Then, a solution of di-*tert* butyl dicarbonate (1.75 eq, 4.97 mmol, 1.08 g) in acetonitrile (25 mL) was added. and the resulting mixture was allowed to stir at room temperature for 16 h. The reaction mixture was evaporated to dryness and purified by flash column chromatography (33% → 50% EtOAc/Heptane) to give the desired product **2** as a yellow solid (639 mg, 2.3 mmol, 81%). **^{1}H NMR** (300 MHz, $CDCl_3$) δ 1.44 (s, 9H), 4.49 (d, J = 5.9 Hz, 2H), 5.24 (br s, 1H, NH), 7.28-7.39 (m, 1H), 7.44 (td, J = 7.9, 5.2 Hz, 1H), 7.55 (app d, J = 8.1 Hz, 1H), 8.04 (s, 1H), 8.87 (d, J = 1.7 Hz, 1H) ppm; 13C NMR (75 MHz, $CDCl_3$) δ 28.5, 42.5, 80.2, 113.4 (d, J (C,F) = 18.9 Hz), 123.4 (d, J (C,F) = 4.7 Hz), 126.8 (d, J (C,F) = 8.1 Hz), 129.6 (d, J (C,F) = 2.2 Hz), 133.2, 133.8, 137.8 (d, J (C,F) = 12.0 Hz), 158.8 (d, J (C,F) = 1.6 Hz), 156.0, 158.1 (d, J (C,F) = 256.9 Hz) ppm.

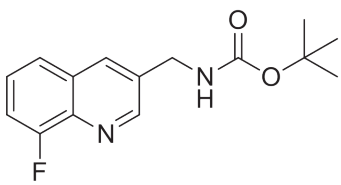

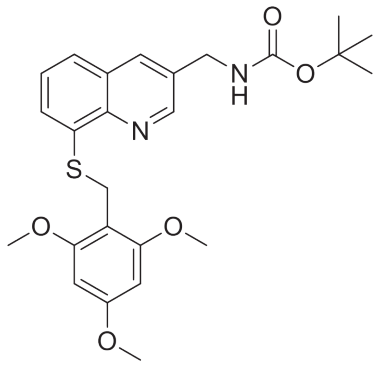

Synthesis of tert-butyl ((8-((2,4,6-trimethoxybenzyl)thio)quinolin-3-yl)methyl)carbamate (3).

To a solution of (2,4,6-trimethoxyphenyl)methanethiol (3 eq, 1.26 g, 5.91 mmol) in dry THF (10 mL) was added NaH (3eq, 236.4 mg, 5.91 mmol) portion wise. To this, a solution of compound **2** (545 mg, 1.97 mmol) in dry THF (10 mL) was added. The resulting mixture was refluxed overnight. After this time, water was added to quench the reaction and the mixture was extracted with EtOAc (3 x 30 mL). The combined organic layers were dried over Na_2SO_4 and concentrated under reduced pressure. The mixture was purified by column chromatography (33% EtOAc/Toluene) to give the desired product 3 as a yellow oil (155 mg, 0.33 mmol, 16.7%). **^{1}H NMR** (300 MHz, $CDCl_3$) δ 1.45 (s, 9H), 2.35 (s, 1H), 3.76 (s, 6H), 3.81 (s, 3H), 4.32 (s, 2H), 4.47 (d, J = 5.9 Hz, 2H), 4.99 (br s, 1H, NH), 6.12 (s, 2H), 7.12-7.28 (m, 1H), 7.41-7.59 (m, 2H), 7.64 (dd, J = 6.9, 1.7 Hz, 1H), 7.97 (d, J = 2.0 Hz, 1H), 8.81 (d, J = 2.2 Hz, 1H) ppm.

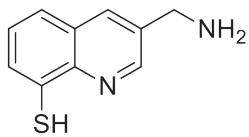

Synthesis of 3-(aminomethyl)quinoline-8-thiol (4).

A 3 mL solution of TFA:TES:H_2O, 95:2.5:2.5 (v/v/v) was added to Compound **3** (135 mg, 0.28 mmol) and left stirring at room temperature for 1 hour. After this, the reaction mixture was co-evaporated with DCM (3 x 30 mL) and freeze dried (CH_3CN/H_2O/AcOH, 65/25/10, v/v/v). The desired compound **4** was obtained pure as a yellow oil (50.8 mg, 0.266 mmol, 95%). **^{1}H NMR** (300 MHz, CD_3OD) δ 4.43 (s, 2H), 7.52 (dd, J = 8.2, 7.5 Hz, 1H), 7.81 (dd, J = 8.3, 1.2 Hz, 1H), 7.90 (dd, J = 7.5, 1.2 Hz, 1H), 8.46 (d, J = 2.3 Hz, 1H), 9.03 (d, J = 2.3 Hz, 1H) ppm.

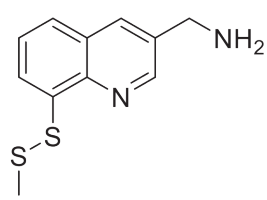

Synthesis of (8-(methyldisulfaneyl)quinolin-3-yl)methanamine (5).

Compound **4** (50.8 mg, 0.266 mmol) dimerized as a disulfide over time and hence the free thiol was protected. Before protecting the thiol, **4** was reduced by adding 1 eq. of ethane-thiol in methanol and left stirring at RT for 3 hours. After total reduction of thiol, 4 eq. S-Methyl methanethiosulfonate (MMTS) was added as a solution to this mixture. The protection of free thiol was followed by LCMS. After complete conversion, the mixture was evaporated and purified over reversed-phase HPLC to yield the desired compound **5** (81%). **^{1}H NMR** (300 MHz, CD_3OD) δ 2.47 (s, 3H), 4.39 (s, 2H), 7.72 (dd, *J* = 8.2, 7.7 Hz, 1H), 7.82 (dd, *J* = 8.3, 1.2 Hz, 1H), 8.22 (dd, *J* = 7.45, 1.2 Hz, 1H), 8.43 (d, *J* = 2.2 Hz, 1H), 8.91 (d, *J* = 2.2 Hz, 1H) ppm. **^{13}C ^{1}H NMR** (75 MHz, $CDCl_3$) δ 151.02, 151.00, 138.79, 138.11, 129.60, 129.23, 128.73, 126.89, 126.69, 49.30, 42.13, 22.53.

Enzyme expression, purification and activity assay

Expression and purification of Rpn11–Rpn8 heterodimers.

A pETDuet-1 vector containing the MPN domains of Rpn11 and Rpn8, a kindly gift from Dr. Andreas Martin, was transformed into BL21 *E.coli* strain. Protocol for expression and purification was described in a previous study.[1] BL21 cells containing Rpn11-Rpn8 expression plasmid were grown in 2xYT medium was supplemented with 150 μM $ZnCl_2$ at 37 ºC until reaches to OD_{600} of about 0.6-0.8. Protein expression was induced with 1mM IPTG and the cells were grown overnight at 18 ºC. Cells were then harvested by centrifugation and lysed with lysis buffer (60 mM HEPES, pH 8.0, 100 mM NaCl, 100 mM KCl, 10% glycerol, 20 mM imidazole, 2 mg/mL lysozyme (Sigma-Aldrich), DNAse I (Roche), and EDTA-free protease inhibitors cocktail tablets (Roche). Further lysis was done by sonication at an amplitude of 60 for 2 min (15 sec pulse-on time and 45 sec pulse-off time) and the cell lysate was clarified by ultracentrifugation at 21,000g for 30 minutes. Soluble cell lysate fraction was incubated with Talon Metal Affinity Resin™ (Clontech) and washed with lysis buffer. Rpn11/Rpn8 heterodimers were eluted with the buffer containing 60 mM HEPES, pH 7.6, 100 mM NaCl, 100 mM KCl, 10% glycerol, and 250 mM imidazole. Eluted proteins were then purified by size-exclusion chromatography on a HiLoad 16/60 Superdex 200 pg column (GE Life Sciences) and then concentrated with a 3K MWCO Amicon Ultra spin filter (Millipore). Purified protein was aliquoted into a small volume and stored at -80 ºC.

Enzyme activity assay:

Ubiquitin-rhodamine assay. The DUB mediated hydrolysis of Ub-rho yields free rhodamine and Ub. The rhodamine signal is measured in a fluorescence intensity assay using a buffer containing 50 mM HEPES, 100 mM NaCl, 100 mM KCl, 1mg/ml CHAPS, 0.1 mM DTT and 0.5 mg/ml BGG at pH 8 and at room temperature. The enzyme (10μL/well) and the substrates (10μL/well) were added to a 384-well Corning™ low volume flat-bottom plates. Fluorescence intensity was monitored at an excitation wavelength of 487 nm and an emission wavelength of 535 nm using EnVision Multilabel Reader, BMG PHERAstar® FSX or BMG CLARIOstar® plate reader. In order to calculate the rate of the enzyme reaction, different concentrations of Rpn11/Rpn8 was added to 2 μM of Ub-rhodamine substrate. The concentration of the hydrolysed product (rhodamine-glycine) was calculated from the fluorescence signal of the free rhodamine-glycine dye after adding 20 nM UCHL3 which ensured the complete hydrolysis of 2 μM of Ub-rhodamine substrate. For general enzyme reactions, the enzyme stock was diluted into the assay buffer at a final concentration of 1 μM. The Ub-rhodamine substrate was prepared synthetically according to the previously reported procedure.[3] The substrate dissolved in DMSO was diluted out in water and later in the assay buffer to a final concentration of 2 μM. The different inhibitor reagents were also prepared as a DMSO stock and diluted out in water and then into the buffer.

Ubiquitin-peptide-TAMRA assay. The DUB-assisted cleavage of Ubiquitin-peptide-TAMRA was followed by fluorescence polarization (FP) in buffer containing 50 mM HEPES, 100 mM NaCl, 100 mM KCl, 1mg/ml CHAPS, 0.1 mM DTT and 0.5 mg/ml BGG at pH 8 and at room temperature. The enzyme (10μL/well) and the substrates (10μL/well) were added to a 384-well Corning™ low volume flat-bottom plates. FP was monitored at 0º and at 90º relative to the polarization of the incident beam at an excitation wavelength of 540

nm and an emission wavelength of 590 nm using BMG PHERAstar® FSX or BMG CLARIOstar® plate reader. Ubiquitin-peptide of different lysine linkages were synthesized according to the procedure described previously. [2] Ubiquitin-TAMRA-K48Ub-peptide (Ub-FP) was used as a substrate in all the FP assays used in this manuscript. The rate of the enzyme activity was calculated by using 1 μM of Rpn11/Rpn8 and 2 μM of the FP assay reagent. Inhibitor reagents were prepared in DMSO as described before. The initial velocity of the enzyme activity was measured as a unit of substrate consumed in the initial part of measurements where the signal is linear. [2]

Computational methodology

The Rpn11/ubiquitin protein complex was constituted using Rpn11 from the Rpn11/Rpn8 complex (PDB: 4O8X) [1] and ubiquitin (PDB: 1UBQ) [4]. Both Rpn11 and ubiquitin were superposed to the structure of AMSH-LP DUB domain in complex with Lys63-linked ubiquitin (PDB: 2ZNV) [5]. The resulting superposed Rpn11/ubiquitin complex was optimized by refining Rpn11 loop-residues 71-84 with Prime [6], followed by molecular dynamic relaxation of the complex. The 8MQ chelator was docked into apo Rpn11 using a constraint for interaction with the Rpn11 pocket zinc atom. The derived 8MQ pose was manually linked to Arg74 from ubiquitin, removing residues 75-76, to construct Ub74. Rpn11 in complex with Ub74 was optimized using molecular dynamics (100 ns) [7]. Other ubiquitin/8MQ chelators were constructed by replacing ubiquitin C-terminus residues with 8MQ manually, followed by optimization using molecular dynamics.

IC_{50} assays

All assay reagents were prepared in the buffer mentioned in the fluorogenic assays described before. For dissolving the inhibitors, the compounds or Ub variants were prepared in DMSO as a stock solution. Then they were dissolved in MQ water and then into one of the fluorogenic assay buffers which contains 25 mM TCEP in order to reduce the protected thiol of the zinc chelating group. Serial dilutions of the inhibitors were prepared in the buffer. After 30 minutes of incubation, the substrate (Ub-rho or UbFP assay reagent) was added centrifuged for 30 secs at 1000 rpm. They are then immediately measured in a plate-reader over a period of up to 90 minutes at RT.

FP binding assay

In a typical FP assay, polarized light at the excitation wavelength is used to excite the fluorogenic molecule. Depending upon the tumbling nature of the molecule, the emitted wavelength is depolarized. This tumbling depends on the binding of the fluorogenic and non-fluorogenic components of the reaction. In our assays, we used rhodamine-labelled Ub-based probes against unlabeled Rpn11/Rpn8 heterodimer. The rho-Ub variants were prepared in DMSO as a stock solution. This was then added to MQ water and then into FP buffer (2μM final concentration) containing 25 mM TCEP to reduce the protected thiol of the zinc chelating group. To this, Rpn11/Rpn8 was added in different concentrations and incubated for 30 minutes at RT. The fluorescence polarization was then measured in a BMG PHERAstar® FSX using end-point measurement and the data was used in GraphPad Prism™ to calculate the binding coefficient.

Enzyme-activity recovery assay

For this assay, 4 μM of the Rpn11/Rpn8 enzyme was pre-incubated with **6** or **10a** at 5 μM and 10 μM respectively for 30 minutes at RT in an FP assay buffer containing 25 mM TCEP to reduce the protected thiol of the zinc chelating group. After this pre-incubation, 10 μM of $ZnSO_4$ was added to the assay buffer containing the enzyme and inhibitor and pre-incubated for another 15 minutes at RT. Later, Ub-K48(TAMRA-peptide) substrate was added and FP was measured over time.

Time-based inhibition assay

In this assay, EDTA, **6**, **10a** and Ub76 were pre-incubated with Rpn11/Rpn8 for different time intervals in an assay buffer containing 25 mM TCEP to reduce the protected thiol of the zinc chelating group. After pre-incubation, the Ub-Rho substrate was added, and the activity of the enzyme was measured in a BMG PHERAstar® FSX for 90 minutes at RT. A graph was plotted with pre-incubation time on the X-axis and rate of the enzyme catalysis on the Y-axis.

Co-elution assay

In this assay, **10b** or Rho-Ub was incubated with Rpn11/Rpn8 in a ratio of 8:1 in a buffer containing 60 mM HEPES, pH 7.6, 100 mM NaCl, 100 mM KCl and 25 mM TCEP. We then used a micro AKTA™ system using native buffer conditions and used an S75/200 column in order to resolve between bound and unbound Rpn11/Rpn8 with **10b**. The eluted fractions were run on a precast 12% NuPAGE Bis-Tris gels on a Novex NuPAGE SDS-PAGE Gel System containing MES buffer. Fluorescence scan was measured on a ProXPRESS 2D Proteomic imaging system (Perkin–Elmer) with a resolution of 100 μm and exposure time of 15 s, with filter settings ($\lambda_{ex}/\lambda_{em}$) 490/540 nm (Rho).

Pull-down assay

HeLa cells were transfected with GFP-POH1, GFP-AMSH, GFP-AMSH-LP and empty GFP vector. After 24 hours, cells were lysed using lysis buffer containing 25 mM HEPES.NaOH (pH 7.4), 50 mM NaCl, 100 mM KCl, NP40 5 mM TCEP and EDTA-free protease inhibitor cocktail (Roche Cat#:5056489001). After centrifugation, the clear lysate was added with **10c** along with other controls like Biotin-8MQ and Biotin-Ub and incubated for 1 hr at RT. Later, Streptavidin beads were added to the lysate and incubated at 4 C for 2 hours. Streptavidin beads were washed with wash buffer cointaning 25 mM HEPES.NaOH (pH 7.4), 50 mM NaCl, 100 mM KCl, NP40 5 mM TCEP. the beads were added with SDS-loading dye containing 10mM DTT. The samples were loaded onto a 10% SDS-PAGE and transferred to nitrocellulose membrane. Antibodies against GFP were used to check for pull-down of GFP-tagged metalloDUBs.

Synthesis of Ub variants

Solid-phase peptide synthesis of Ub

The synthesis of ubiquitin by solid-phase peptide synthesis was carried out according to the previously reported protocol. [3] Ubiquitin (1-74) and Ub (w.t.) were synthesized by solid-phase peptide synthesis on TentaGel Trt R resin. In the case of Rhodamine labelled Ub variants, Rhodamine was coupled on-resin to the N-terminal end of Ub variant by standard chemical coupling. For coupling compound **5** (Scheme **1**) to the C-terminal end of Ub (1-74), the Ub variant was cleaved from resin in a fully-protected version using 20% HFIP in DCM.

After co-evaporating HFIP under reduced pressure, the protected Ub variant was obtained as a colourless oil. In the case of full-length Ub, TFA cleavage mix containing TFA: H_2O: TiPS: Phenol (92.5/2.5/2.5/2.5 v/v/v/v) was used to fully deprotect Ub. The final compound was precipitated in the dry ice cold ether:pentane (3:1) mix and later on lyophilized to yield crude powder which was then purified over reversed-phase HPLC.

Synthesis of Ub_{76}-NHOH and Ub_{75}-NHOH

Ubiquitin was synthesized in a linear fashion in the same way as described before. Fmoc-hydroxylamine was coupled to chlorotrityl-chloride resin using PyBOP and DiPEA. After checking the loading of resin, the rest of the peptides based on the sequence of Ub (1-75) or Ub (1-76) were synthesized using SPPS. After global deprotection, the final product was obtained as Ub_{76}-NHOH and Ub_{75}-NHOH as confirmed by LCMS analysis. (**Figure S21 and S22**)

Synthesis of Ub-8MQ-SMe (10a)

Ub (1-74) was synthesized on a TentaGel Trt R resin. After cleaving the protected peptide from the resin by treating the resin with 20% HFIP in DCM, the C-terminus of Ub74 was coupled in solution to compound **5** using 4 eq each of HOBT and HBTU and 8 eq of DiPEA, in order to minimize racemization problems associated with coupling to side-chain containing amino acids. [8, 9] The reaction mix was left overnight and checked by LCMS for the full conversion into the product. After confirming the formation of the product, the final compound was subjected to global deprotection using TFA cleavage mix mentioned before, precipitated in the dry ice cold ether: pentane, and finally lyophilized as a powder.

Synthesis of Rho-Ub-8MQ-SMe (10b)

Rhodamine was attached to the N-terminal of linearly synthesized ubiquitin on resin using standard coupling conditions containing 4 eq PyBOP, 4 eq Rhodamine diBoc and 8 eq DiPEA. After this, the protected ubiquitin was cleaved off the resin using 20% HFIP in DCM and co-evaporated. [10] Compound **5** was attached to the C-terminal end using the procedure mentioned before.

Synthesis of Bio-$(PEG)_2$-Ub-8MQ-SMe (10c)

First, Fmoc-$(PEG)_2$ was attached to the N-terminal of linearly synthesized ubiquitin on resin using standard coupling conditions containing 4 eq PyBOP, 4 eq Biotin and 8 eq DiPEA. The Fmoc is then cleaved using 20% piperidine in NMP. Next, Biotin was coupled on the N-terminus of $(PEG)_2$-Ub on the resin. After this, the protected ubiquitin was cleaved off the resin using 20% HFIP in DCM and co-evaporated. [10] Compound **5** was attached to the C-terminal end using the procedure mentioned before.

Synthesis of Biotin-$(PEG)_2$-8MQ

Biotin-$(PEG)_2$ was initially prepared by coupling Fmoc-(PEG)2 on Chloro-trityl chloride resin with a loading of 0.4 g/Mol. Fmoc was removed using 20% piperidine in NMP. Biotin was then coupled on the N-terminus of $(PEG)_2$ using 4 eq PyBOP, 4 eq Biotin and 8 eq DiPEA, overnight. The resulting Biotin-(PEG)2 was cleaved from the resin using TFA cleavage mix mentioned in the standard procedure. Compound **5** was attached to the C-terminal end using the procedure mentioned before. The product was then purified using reverse-phase HPLC to obtain Biotin-$(PEG)_2$-8MQ.

Preparation of sample for HPLC purification

All Ub variants were first dissolved in DMSO. This solution was slowly added to MQ water containing 0.05% TFA and filtered through a GfxO/0.45µm GHP membrane Acrodisc® Premium 25mm syringe filter. The sample was then injected onto a Waters XBridge™ Prep C18 Column (30 x 150 mm, 5µm OBD™) at a flow rate of 37.5 ml/min. The protein was purified with the gradient outlined in the table below using aq. 0.05% TFA (Solvent A) and acetonitrile containing 0.05% TFA (Solvent B) as eluents.

Time (in mins)	Solvent B (%)
0 ⇨ 5	5
5 ⇨ 7	5 ⇨ 25
7 ⇨ 22	25 ⇨ 55
22 ⇨ 24	55 ⇨ 95
24 ⇨ 27	95
27 ⇨ 27.5	95 ⇨ 5
27.5 ⇨ 30	5

The retention time for the ubiquitin variants was approximately 10 minutes. All fractions containing the protein were confirmed by checking the mass using a LC-MS R_t 2.8 min; Phenomenex Kinetex™ XB-C18 100A (50 x 2 x 10 mm, 2.6 µm); solvents - MQ water with 0.1% formic acid (Solvent A) and acetonitrile containing 0.1% formic acid (Solvent B), flow rate = 0.5 mL/min, run time = 6 min, column T = 45°C. Gradient: 5% ⇨ 95% B over 3.5 min. All samples containing pure protein were pooled together and lyophilized.

Analysis of purified ubiquitin variants

The ubiquitin variants were dissolved in DMSO to a concentration of 10 mg/mL. 0.5 µL of this sample was resuspended in 100 µL MQ water. This was then used in LCMS analysis using LCT Premiere™ mass spectroscopy analysis.

The LC-MS analysis of the purified reagents

All purified proteins were confirmed by checking the mass using LC-MS. Phenomenex Kinetex™ C18 (100A, 100 x 21 mm, 2.6 µm); solvents – aq. 0.1% formic acid (Solvent A) and acetonitrile containing 0.1% formic acid (Solvent B), flow rate = 0.4 mL/min, runtime = 13 min, column T = 45°C. Gradient: 5% ⇨ 95% B over 7.6 min.

1. Zinc chelating molecule (5)

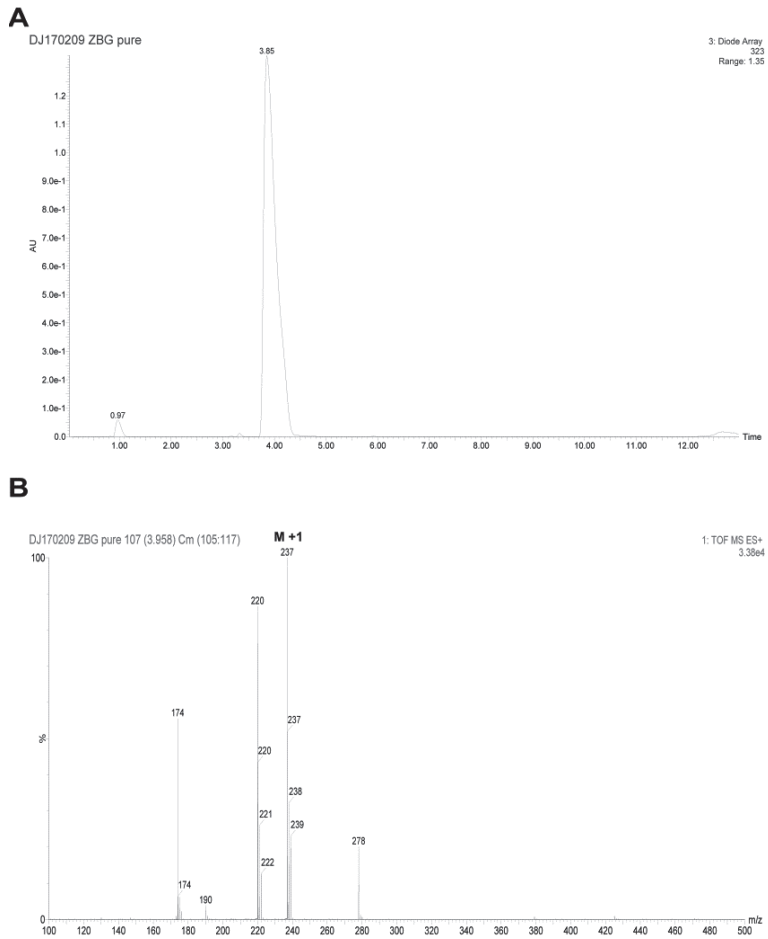

Figure S13: *Analytical data for the synthesized zinc chelator (Compound* ***5****).* ***A:*** *UV chromatogram (λ - 323 nm) using LC-MS;* ***B:*** *Spectrum of the peak at 3.85 min; ESI-Mass [M+H] Expected: 237.35 / Found: 237.*

2. Ub-8MQ (10a, reduced)

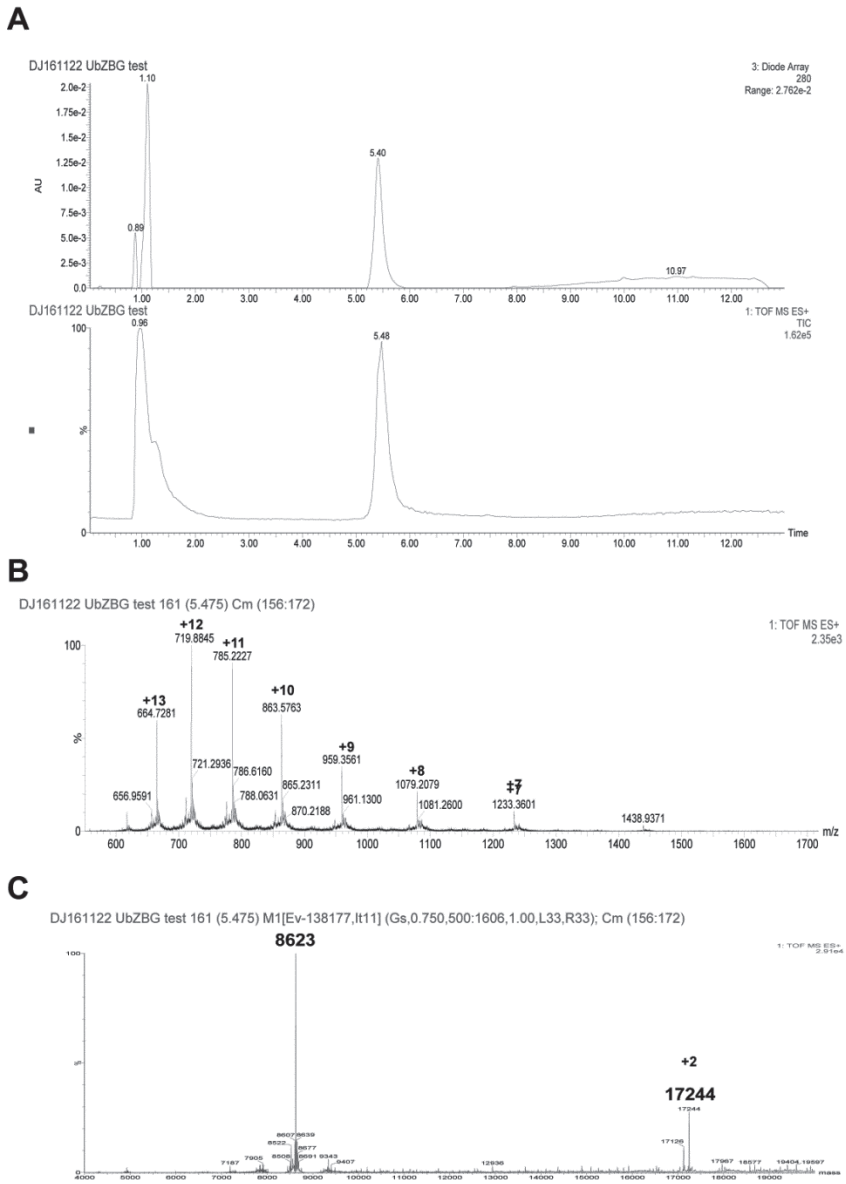

Figure S14: *Ub-8MQ.* ***A:*** *Top: UV chromatogram (λ - 280 nm); Bottom: combined mass spectrum using LC-MS;* ***B:*** *Spectrum of the peak at 5.40 min;* ***C:*** *Deconvoluted mass of peak spectra. ESI-Mass [M+H] Expected: 8622.9 / Found:* ***M+1H*** *= 8623;* ***M+2H*** *= 17244.*

3. Ub-8MQ-SMe (10a)

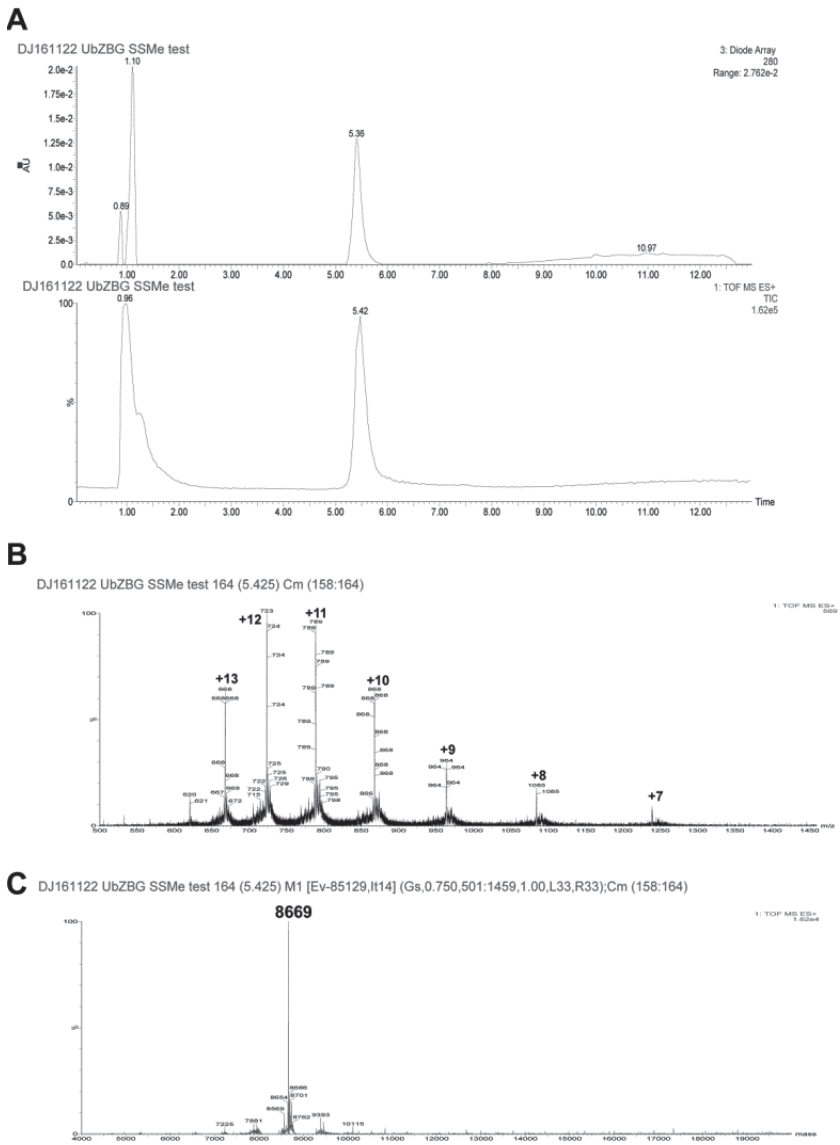

Figure S15:*Ub-8MQ-SMe (**9a**). **A:** Top: UV chromatogram (λ - 280 nm); Bottom: combined mass spectrum using LC-MS; **B:** Spectrum of the peak at 5.36 min; **C:** Deconvoluted mass of peak spectra. ESI-Mass [M+H] Expected: 8667.9 / Found: 8669.*

4. RhoUb-8MQ-SMe (10b)

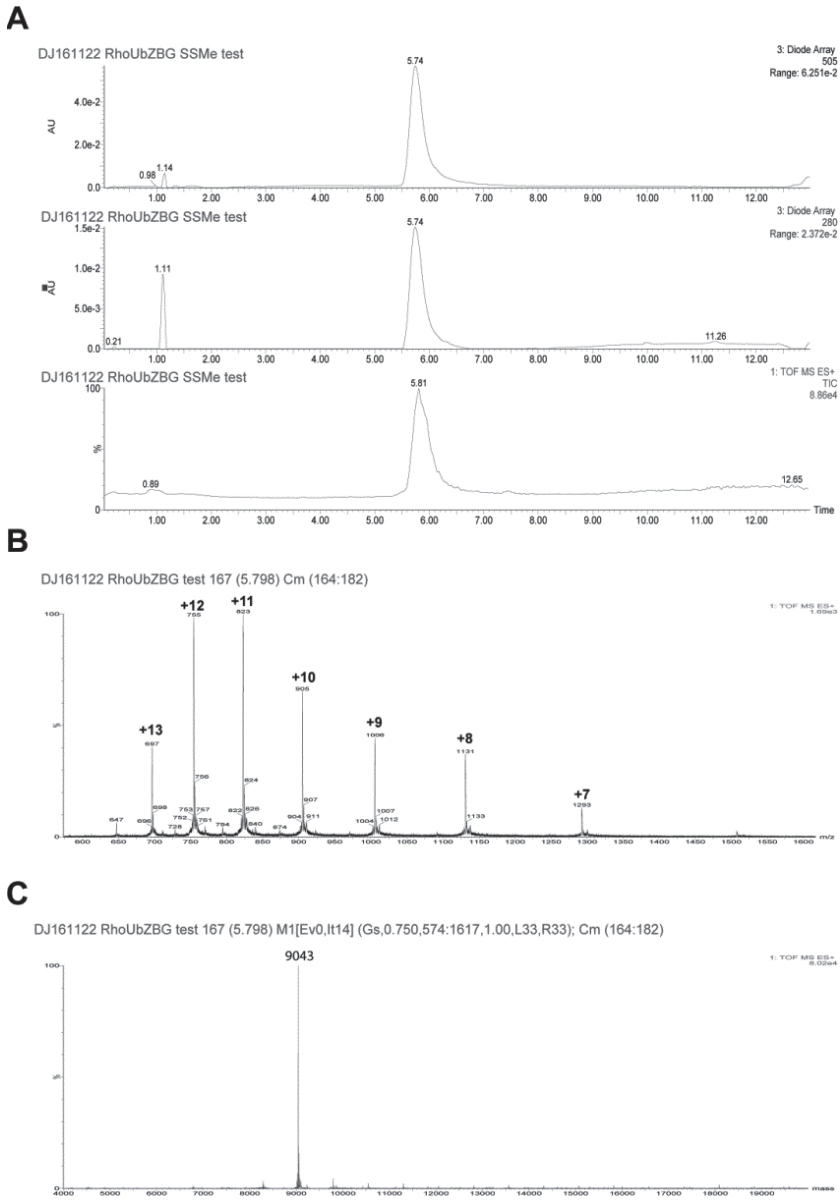

Figure S16: *RhoUb-8MQ-SMe (**9b**). **A:** Top: UV chromatogram (λ - 505 nm); Middle: UV chromatogram (λ - 280 nm); Bottom: combined mass spectrum using LC-MS; **B:** Spectrum of the peak at 5.74 min; **C:** Deconvoluted mass of peak spectra. ESI-Mass [M+H] Expected: 9042.9 / Found: 9043.*

5. RhoUb

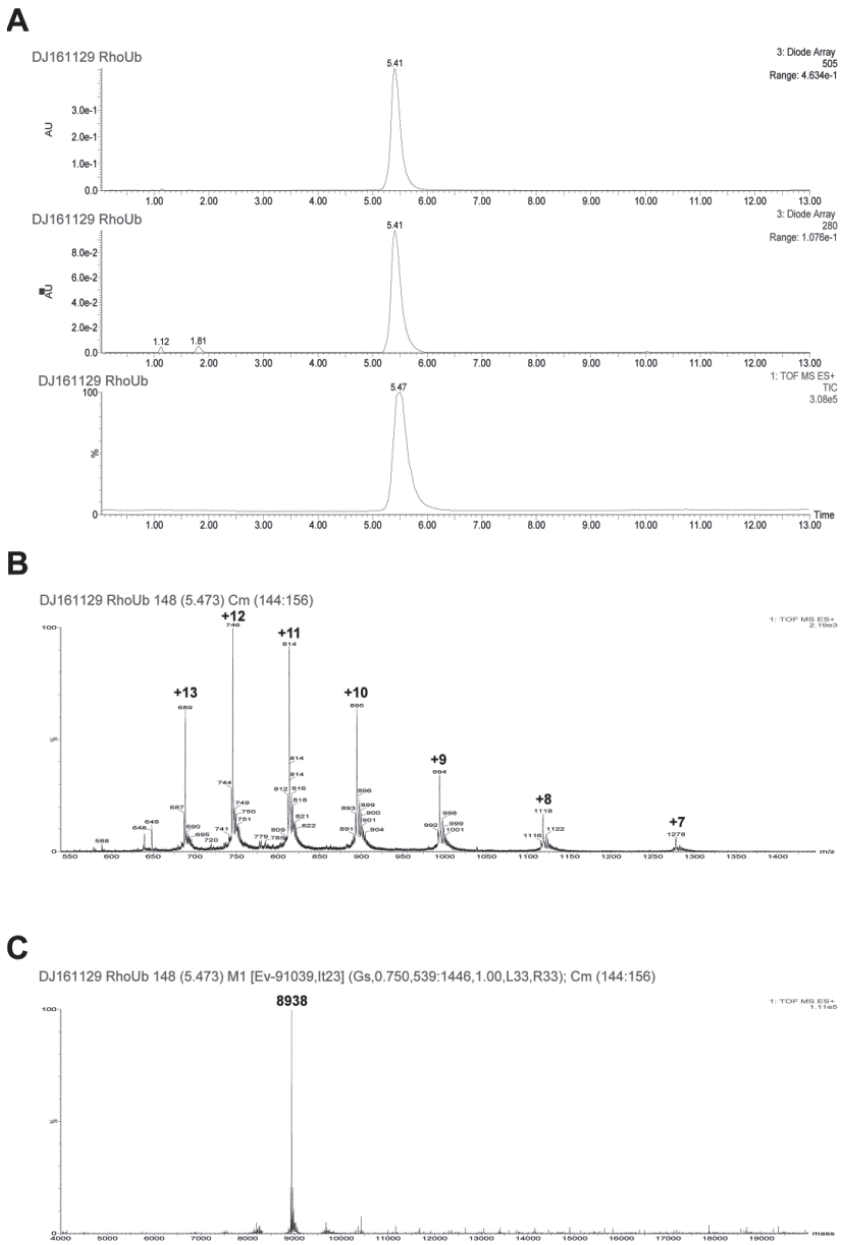

Figure S17: *RhoUb.* ***A:*** *Top: UV chromatogram (λ - 505 nm); Middle: UV chromatogram (λ - 280 nm); Bottom: combined mass spectrum using LC-MS;* ***B:*** *Spectrum of the peak at 5.41 min;* ***C:*** *Deconvoluted mass of peak spectra. ESI-Mass [M+H] Expected: 8938.9 / Found: 8938.*

6. Biotin-(PEG)$_2$-Ub8MQ-SMe (10c)

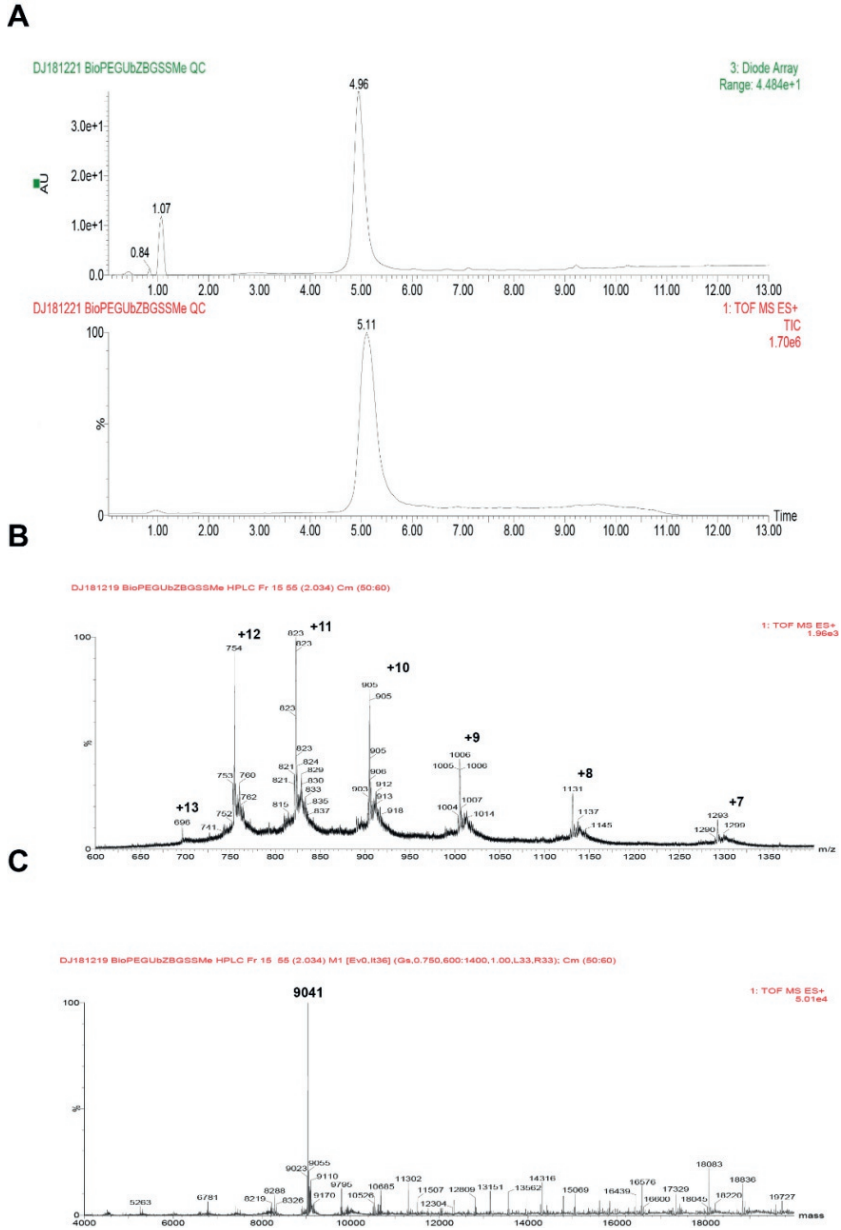

Figure S18: *Biotin-(PEG)$_2$-Ub-8MQ-SMe.* ***A:*** *Top: UV chromatogram (λ - 280 nm); Bottom: combined mass spectrum using LC-MS;* ***B:*** *Spectrum of the peak at 5.11 min;* ***C:*** *Deconvoluted mass of peak spectra. ESI-Mass [M+H] Expected: 9042.2 / Found: 9041.*

7. Biotin-(PEG)$_2$-8MQ-SMe

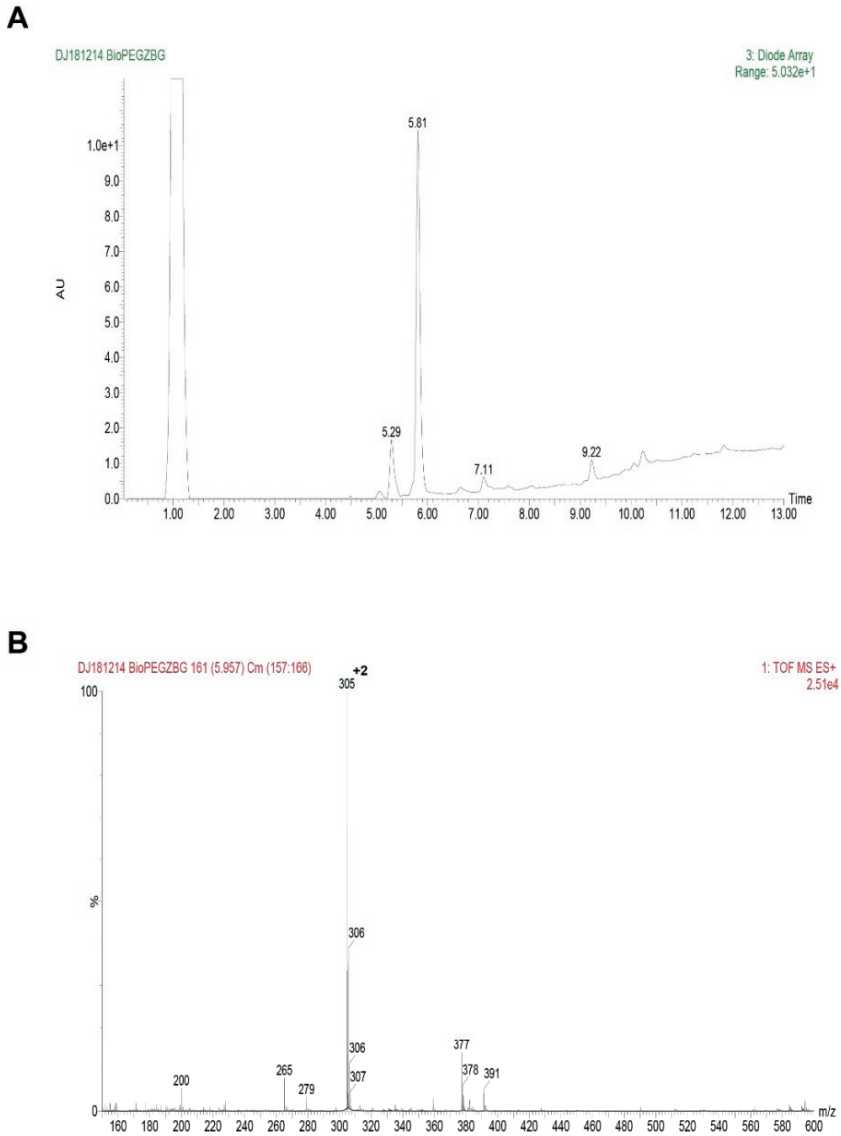

Figure S19: *Biotin-(PEG)$_2$- 8MQ-SMe.* ***A:*** *UV chromatogram (λ - 280 nm);* ***B:*** *Spectrum of the peak at 5.81 min; ESI-Mass [M+2H] Expected: 305.7 / Found: 305.*

8. Biotin-(PEG)$_2$-Ub

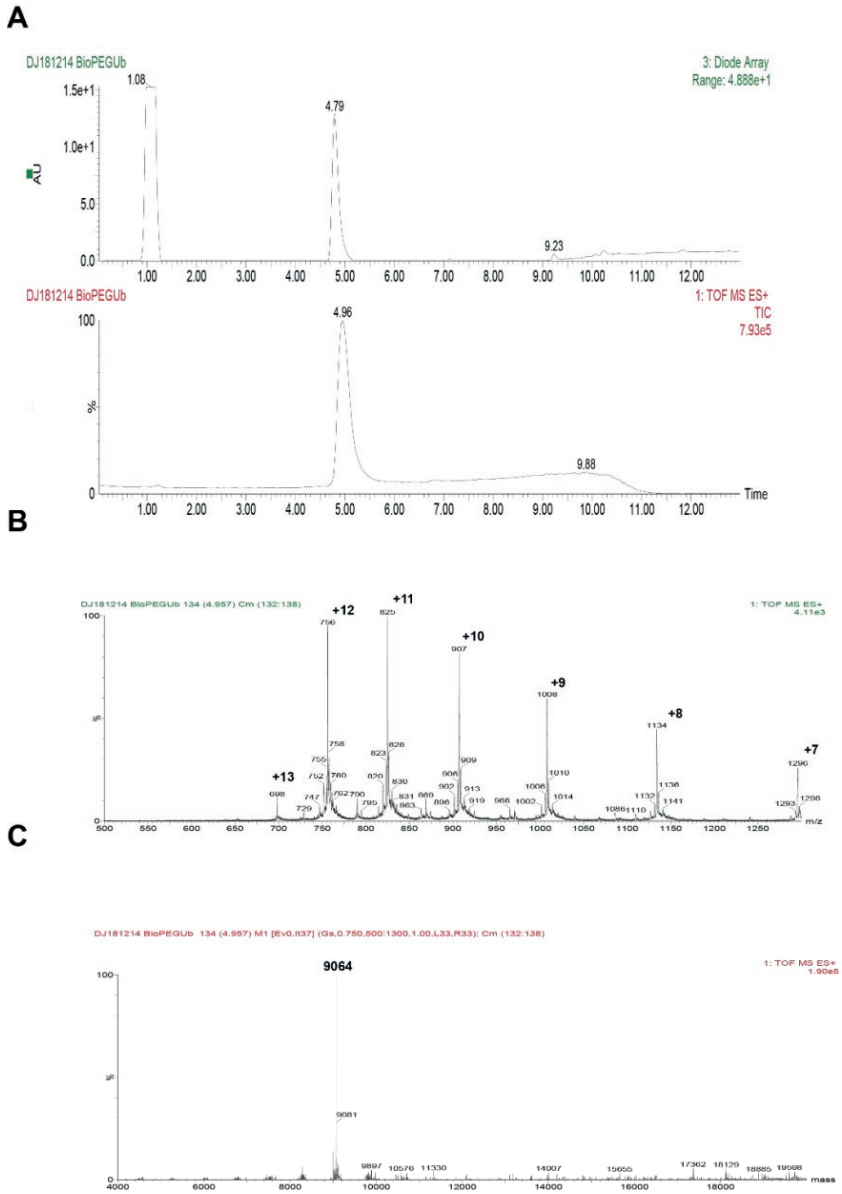

Figure S20: *Biotin-(PEG)$_2$-Ub.* ***A:*** *Top: UV chromatogram (λ - 280 nm); Bottom: combined mass spectrum using LC-MS;* ***B:*** *Spectrum of the peak at 4.96 min;* ***C:*** *Deconvoluted mass of peak spectra. ESI-Mass [M+H] Expected: 9065.6 / Found: 9064.*

9. Ub_{76}-NHOH

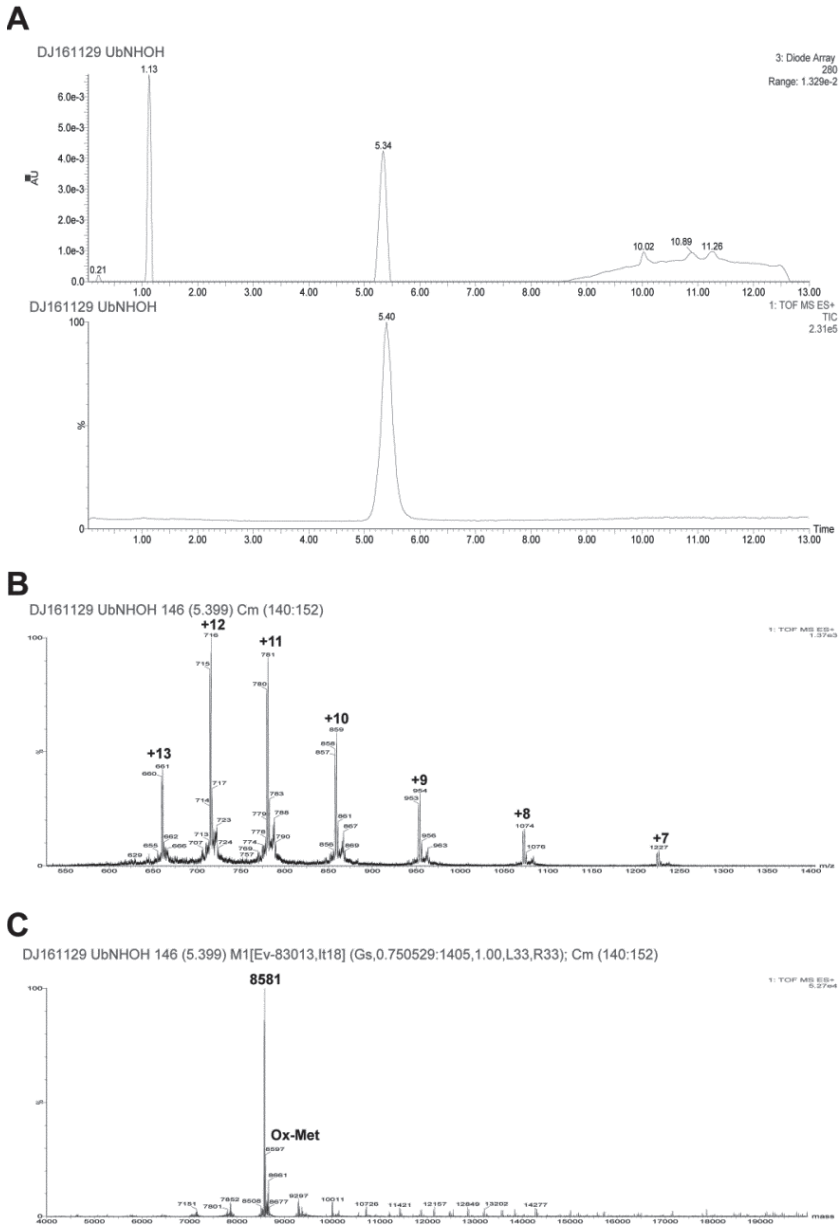

Figure S21: *Ub_{76}NHOH.* ***A:*** *Top: UV chromatogram (λ - 280 nm); Bottom: combined mass spectrum using LC-MS;* ***B:*** *Spectrum of the peak at 5.34 min;* ***C:*** *Deconvoluted mass of peak spectra. ESI-Mass [M+H] Expected: 8579.9 / Found: 8581; Oxidized-Methionine Ub_{76}NHOH mass: 8597.*

10. Ub_{75}-NHOH

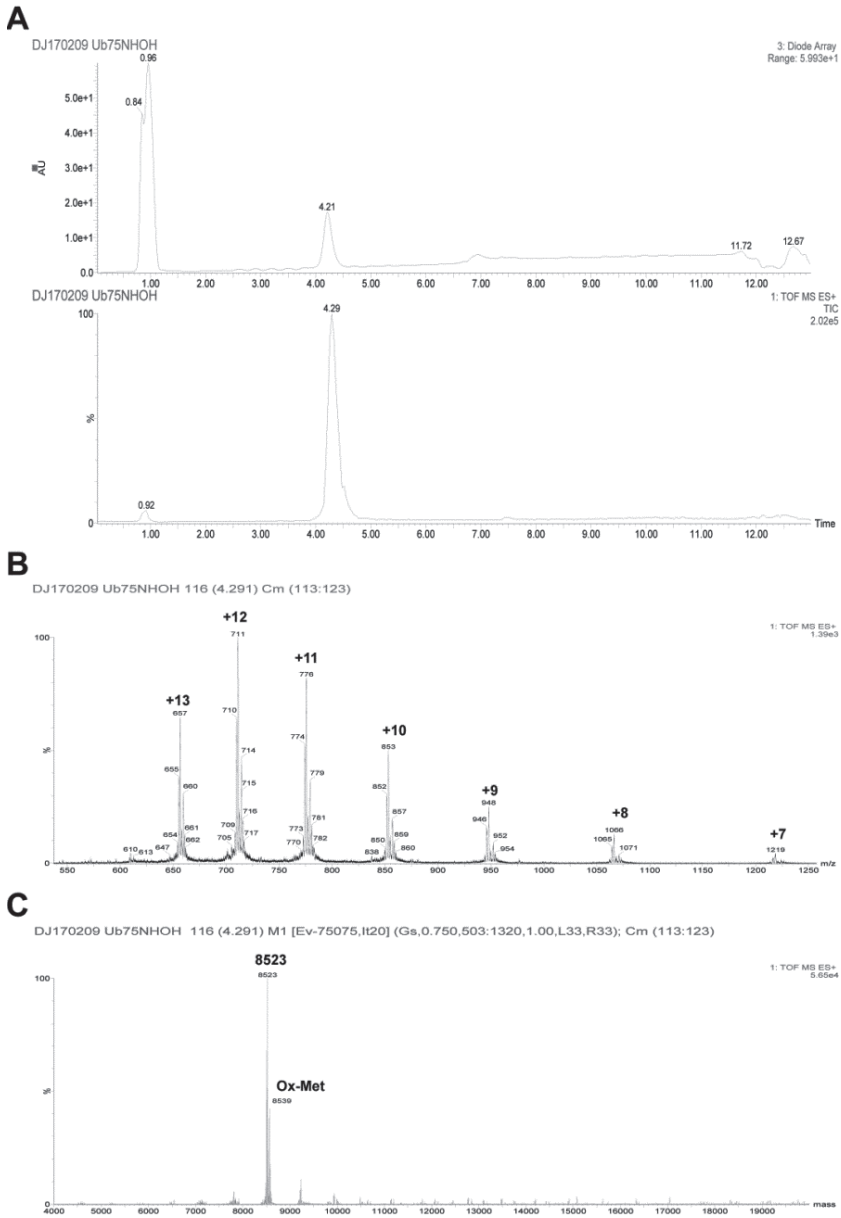

Figure S22: *Ub_{75}NHOH.* ***A:*** *Top: UV chromatogram (λ - 280 nm); Bottom: combined mass spectrum using LC-MS;* ***B:*** *Spectrum of the peak at 5.34 min;* ***C:*** *Deconvoluted mass of peak spectra. ESI-Mass [M+H] Expected: 8521.9 / Found: 8523; Oxidized-Methionine Ub_{75}NHOH mass: 8539.*

Supplementary References

1. Worden, E.J., C. Padovani, and A. Martin, *Structure of the Rpn11-Rpn8 dimer reveals mechanisms of substrate deubiquitination during proteasomal degradation.* Nat Struct Mol Biol, 2014. **21**(3): p. 220-7.
2. Geurink, P.P., et al., *A general chemical ligation approach towards isopeptide-linked ubiquitin and ubiquitin-like assay reagents.* Chembiochem, 2012. **13**(2): p. 293-7.
3. El Oualid, F., et al., *Chemical synthesis of ubiquitin, ubiquitin-based probes, and diubiquitin.* Angew Chem Int Ed Engl, 2010. **49**(52): p. 10149-53.
4. Vijay-Kumar, S., C.E. Bugg, and W.J. Cook, *Structure of ubiquitin refined at 1.8 A resolution.* J Mol Biol, 1987. **194**(3): p. 531-44.
5. Sato, Y., et al., *Structural basis for specific cleavage of Lys 63-linked polyubiquitin chains.* Nature, 2008. **455**(7211): p. 358-62.
6. *Schrödinger Release 2017-4: Prime, Schrödinger, LLC, New York, NY, 2017*.
7. *Schrödinger Release 2017-4: Desmond Molecular Dynamics System, D. E. Shaw Research, New York, NY, 2017. Maestro-Desmond Interoperability Tools, Schrödinger, New York, NY, 2017.*
8. Knorr, R., et al., *New coupling reagents in peptide chemistry.* Tetrahedron Letters, 1989. **30**(15): p. 1927-1930.
9. Xiao, N., Z.X. Jiang, and Y.B. Yu, *Enantioselective synthesis of (2R, 3S)- and (2S, 3R)-4,4,4-trifluoro-N-Fmoc-O-tert-butyl-threonine and their racemization-free incorporation into oligopeptides via solid-phase synthesis.* Biopolymers, 2007. **88**(6): p. 781-96.
10. Geurink, P.P., et al., *Development of Diubiquitin-Based FRET Probes To Quantify Ubiquitin Linkage Specificity of Deubiquitinating Enzymes.* Chembiochem, 2016. **17**(9): p. 816-20.